Cell Death and Differentiation (2004) 11, 512–526

www.nature.com/cdd

Human αA- and αB-crystallins bind to Bax and Bcl-X_S to sequester their translocation during staurosporine-induced apoptosis

Y-W Mao[1,4], J-P Liu[2], H Xiang[1,5] and D W-C Li*[,1,2,3]

[1] Department of Molecular Biology, University of Medicine and Dentistry of New Jersey, Stratford, NJ, USA
[2] Hormel Institute, University of Minnesota, Austin, MN, USA
[3] College of Life Sciences, Hunan Normal University, Changsha, Hunan, China
[4] Current address: Department of Pharmacology, University of Michigan, Ann Arbor, MI 48109, USA
[5] Current address: State Key Laboratory of Microbial Resources and Center for Molecular Microbiology, Institute of Microbiology, Chinese Academy of Sciences, Beijing 100080, PR China
* Corresponding author: D W-C Li, Hormel Institute, University of Minnesota, 801 16th Avenue NE, Austin, MN 55912, USA. Tel: + 507-437-9636; Fax: + 507-437-9606; E-mail: dwcli@hi.umn.edu

Received 25.7.03; revised 14.11.03; accepted 19.11.03; published online 30.1.04
Edited by Dr M Piacentini

Abstract

αA- and αB-crystallins are distinct antiapoptotic regulators. Regarding the antiapoptotic mechanisms, we have recently demonstrated that αB-crystallin interacts with the procaspase-3 and partially processed procaspase-3 to repress caspase-3 activation. Here, we demonstrate that human αA- and αB-crystallins prevent staurosporine-induced apoptosis through interactions with members of the Bcl-2 family. Using GST pulldown assays and coimmunoprecipitations, we demonstrated that α-crystallins bind to Bax and Bcl-X_S both *in vitro* and *in vivo*. Human αA- and αB-crystallins display similar affinity to both proapoptotic regulators, and so are true with their antiapoptotic ability tested in human lens epithelial cells, human retina pigment epithelial cells (ARPE-19) and rat embryonic myocardium cells (H9c2) under treatment of staurosporine, etoposide or sorbitol. Two prominent mutants, R116C in αA-crystallin and R120G, in αB-crystallin display much weaker affinity to Bax and Bcl-X_S. Through the interaction, α-crystallins prevent the translocation of Bax and Bcl-X_S from cytosol into mitochondria during staurosporine-induced apoptosis. As a result, α-crystallins preserve the integrity of mitochondria, restrict release of cytochrome *c*, repress activation of caspase-3 and block degradation of PARP. Thus, our results demonstrate a novel antiapoptotic mechanism for α-crystallins.

Cell Death and Differentiation (2004) **11,** 512–526.
doi:10.1038/sj.cdd.4401384
Published online 30 January 2004

Keywords: αA-crystallin; R116C; αB-crystallin; R120G; Bax; Bcl-X_S

Abbreviations: α-crystallin, alpha-crystallin; GFP, green fluorescence protein; HαA, human αA-crystallin; HαB, human αB-crystallin; GFP-HαA, green fluorescence and human αA-crystallin fusion protein; GFP-HαB, green fluorescence and human αB-crystallin fusion protein; MEM, Eagle's minimal essential medium; PAGE, polyacrylamide gel electrophoresis; PBS, phosphate-buffered saline; PMSF, phenylmethylsufonyl fluoride; HLE, human lens epithelial cells; SDS, sodium dodecylsulfate; TBS, tris-buffered saline; TBS-T, tris-buffered saline with tween-20.

Introduction

Apoptosis is one of the major causes for ocular diseases. [1–3] In lens system, our previous work[4–6] has suggested that induced lens epithelial cell apoptosis appears to be a common cellular mechanism mediating stress-induced, noncongenital cataractogenesis. Subsequently, several laboratories have reported that lens epithelial cell apoptosis is indeed actively involved in lens pathogenesis as demonstrated from *in vivo* animal model studies.[7–12] In addition, both overexpression of various exogenous genes and disruption of certain endogenous genes also lead to lens cell apoptosis followed by abnormal lens formation during lens development.[13–18]

Apoptosis is regulated by a series of positive and negative regulators. The balance of these regulators controls the determination of apoptosis. Among these various apoptotic regulators, members of Bcl-2 family and heat-shock proteins play an important role.[19–21]

So far, members of the Bcl-2 family are the most well-characterized apoptotic regulators and are generally classified into two functional groups.[21] Members of the first group, including Bcl-2 and Bcl-X_L, possess antiapoptotic ability, while members of the second group such as Bak, Bax and Bcl-X_S have been shown to promote apoptosis.[21] The functions of Bcl-2 family members could be regulated by their subcellular localization. Bcl-2 and Bcl-X_L are localized on the mitochondrial membrane, endoplasmic reticulum (ER) and nuclear membrane.[21,22] In contrast, a substantial fraction of Bax is found in the cytosol and loosely attached to the mitochondrial membrane prior to induction of cell death.[23] In the absence of death stimuli, the N-terminus of Bax helps to maintain the inactive status of Bax by restraining the C-terminal transmembrane (TM) domain in the cytosol.[24] Lack of the N-terminus of Bax or replacement of the TM domain of Bax with the corresponding domain of Bcl-2 permits the integration of Bax into the mitochondrial membrane.[25] The C-terminal TM domain of Bax is critical for its targeting to mitochondrial membrane. Deletion and point mutations of the C-terminal hydrophobic region severely damage the ability of Bax to integrate into the mitochondrial membrane and kill cells.[26] During apoptosis, Bax undergoes a conformational change that enables it to insert into the mitochondrial outer membrane.[24] Stimulated by death signals, the C-terminal domain

of Bax changes its conformation and the C-terminal α-helix is removed from the BH3 domain, which allows the BH3 domain to interact with other antiapoptotic Bcl-2 family members.[27,28] Caspase[25] and p38 MAP kinase[29] may stimulate the translocation of Bax upon apoptotic stimulus. After Bax inserts into the mitochondrial membrane, Bax can directly induce the release of cytochrome *c*[30,31] or form permeability transition pore.[32]

Bcl-X_S is a proapoptotic regulator with only the BH3, BH4 and TM domains.[33] Several reports have demonstrated that overexpression of Bcl-X_S selectively induces tumor cells to undergo apoptosis.[34–35] Moreover, overexpression of Bcl-X_S in the skin of transgenic mice results in extreme sensitivity to UV-induced cell death.[36] Bcl-X_S has been suggested to stimulate apoptosis through inactivation of antiapoptotic Bcl-2 family members, such as Bcl-2 and Bcl-X_L,[33] or repression of the binding of Bcl-X_L to cytochrome *c*.[37] The endogenous Bcl-X_S is distributed in the cytosol, but is translocated to the mitochondrial membrane upon overexpression. Its proapoptotic ability can be inhibited by Bcl-2 and Bcl-X_L.[38]

Another important group of apoptosis regulators are heat-shock proteins that include alpha-crystallins (α-crystallins),[39–46] Hsp27,[39–40, 47–52] Hsp70,[53–57] Hsp90[58] and Hsp60.[59–60] While Hsp60 appears to enhance apoptosis by promoting maturation of procaspase-3,[59,60] the majority of these factors seems to protect cells from induced apoptosis through different mechanisms. Hsp90 is able to inhibit apoptosome formation.[58] Hsp70 can interact with BAG-1[57,58] and inhibit apoptosis by preventing recruitment of procaspase-9 to the Apaf-1 apoptosome complex.[53] Hsp70 is also capable of functioning downstream of caspase activation.[54] Hsp27 prevents cell death at multiple signaling steps. First, it interacts with cytochrome *c* to prevent activation of procaspase-9.[47,48] It also binds to caspase-3 and modulates the activity of caspase-3.[49] Finally, Hsp27 can abrogate apoptotic pathway through regulation of Bid intracellular distribution and protection of F-actin integrity.[52]

Both α-crystallins and Hsp27 are closely related family members.[19–20,61] αA/B-crystallins are initially known as major lens structural proteins that play an essential role in maintaining the transparency of the ocular lens.[62] Later, α-crystallins are found to act as molecular chaperones[63–67] and also display autokinase activity.[68,69] As antiapoptotic regulators, α-crystallins are initially shown to protect cells from thermal,[70] osmotic[71] and oxidative insult.[72] More recently, α-crystallins have been shown to prevent induced apoptosis by various factors including staurosporine,[39–40,43] TNF,[39,43] UVA irradiation,[43] okadaic acid[44] and hydrogen peroxide.[45] Regarding the antiapoptotic mechanism, recent studies from our laboratory and another group have demonstrated that αB-crystallin can directly interact with the precursors of caspase-3 to suppress its activation.[45,46]

In the present study, we have explored the interactions between α-crystallins and members of the Bcl-2 family. Our results demonstrated that human αA- and αB-crystallins (HαA and HαB) can directly bind to Bax and Bcl-X_S *in vitro* and *in vivo*. The two crystallins display almost close affinity to both proapoptotic regulators, and so are true with their antiapoptotic ability tested in three different cell lines under treatment of different stress conditions. The two prominent mutants, R116C in αA-crystallin and R120G in αB-crystallin, displayed much weaker affinity to Bax and Bcl-X_S. The two crystallins markedly sequestered Bax and Bcl-X_S in the cytosol and prevented their translocation into mitochondria during staurosporine-induced apoptosis. In contrast, the two mutants only weakly sequestered Bax and Bcl-X_S in the cytoplasm. As a result of this interaction, the two crystallins preserve the integrity of mitochondria and turn off the downstream apoptotic events. Thus, our results provide a novel antiapoptotic mechanism for αA/B-crystallins.

Results

Expression of human α-crystallins in human lens epithelial (HLE) cells

To study the mechanisms by which α-crystallins protect lens epithelial cells from stress-induced apoptosis, we cloned both αA- and αB-crystallin cDNAs from human eye lenses (National Disease Research Interchange). Then, we generated the in frame constructs expressing fusion proteins of HαA and HαB with green fluorescence protein (GFP). These expression constructs (pEGFP-HαA and pEGFP-HαB) and the vector (pEGFP-neo) were transfected into the HLE cells using electroporation.[44,45] The stable expression clones of pEGFP-HLE (expressing only GFP from the vector), pEGFP-HαA-HLE (expressing GFP-HαA) and pEGFP-HαB-HLE (expressing GFP-HαB) were obtained after a 6-week selection with G418 (600 μg/ml). As shown in Figure 1, expression of GFP, green fluorescence and human αA-crystallin fusion protein (GFP-HαA) and green fluorescence and human αB-crystallin fusion protein (GFP-HαB) can be detected by fluorescence microscopy. The GFP was distributed homogeneously throughout the nucleus and cytoplasm (Figure 1a). In contrast, the GFP-HαA (Figure 1b) and GFP-HαB (Figure 1c) were localized in the cytoplasm only. Western blot analysis was conducted to further confirm the expression of these proteins. As shown in Figure 1d (top panel), the anti-αA/B-crystallin antibody recognized the GFP-HαA in pEGFP-HαA-HLE cells and GFP-HαB in pEGFP-HαB-HLE cells, respectively. Expression of the endogenous HαA or HαB was hardly detectable in all three types of cells (data not shown). When anti-GFP antibody was used to probe the same blot (the second panel from the top of Figure 1d), the same GFP-HαA and GFP-HαB were detected in pEGFP-HαA-HLE and pEGFP-HαB-HLE cells, respectively. In pEGFP-HLE cells, however, anti-GFP antibody recognized only the 27 kDa GFP protein. As a control for equal loading, the anti-β-actin antibody was used to probe the same blot and the results are shown in the third panel from the top of Figure 1d. Thus, the three different cell lines, pEGPF-HLE, pEGFP-HαA-HLE and pEGFP-HαB-HLE, were successfully established. To quantitate the expression of GFP, GFP-HαA and GFP-HαB in pEGFP-HLE, pEGFP-HαA-HLE and pEGFP-HαB-HLE cells, respectively, purified GFP protein of different concentrations was loaded into the same gel for comparison (bottom panel). After probing with anti-GFP antibody, it was determined that the clone of pEGFP-HLE cells contained about 0.5 ng GFP/μg total proteins, that the clone of pEGFP-HαA-HLE cells expressed about 0.48 ng GFP-HαA/μg total proteins and that

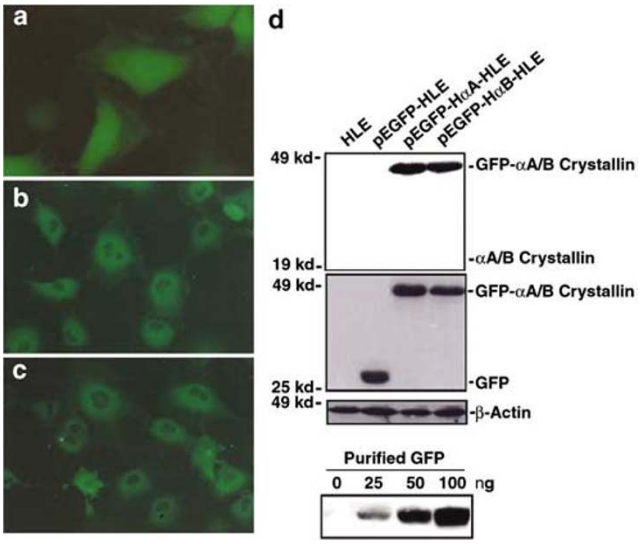

Figure 1 Overexpression of HαA or HαB in HLE cells. (**a-c**) Direct visualization of the pEGFP-HLE, pEGFP-HαA-HLE and pEGFP-HαB-HLE cells by fluorescence microscopy. Note that in the vector-transfected cells (**a**), the GFP protein is homogeneously expressed in both cytoplasm and nucleus. In contrast, in either HαA (**b**)- or HαB (**c**)-transfected cells, the fusion protein of GFP-HαA or GFP-HαB was only detected in the cytoplasm. (**d**) Western blot analysis of HαA and HαB in parental, pEGFP-HLE, pEGFP-HαA-HLE and pEGFP-HαB-HLE. Total proteins (100 μg) from the four types of cells were separated by 10% SDS polyacrylamide gel and transferred to nitrocellulose membrane. Then the membrane was blotted sequentially with anti-αA/B-crystallin antibody (top panel), anti-GFP antibody (middle panel) and anti-β-actin antibody (bottom panel) and visualized with the ECM Kit (Amersham). The purified GFP (bottom panel, from Clontech) was loaded in the same gel and used for reference to measure the concentrations of GFP, GFP-HαA and GFP-HαB in pEGFP-HLE, pEGFP-HαA-HLE and pEGFP-HαB-HLE cells, respectively. Note that the endogenous α-crystallin was hardly detectable in any of the four types of cells (top panel)

the clone of pEGFP-HαB-HLE cells had about 0.42 ng GFP-HαB/μg total proteins.

HαA- and HαB-crystallins prevent staurosporine-induced apoptosis in HLE cells

Our previous studies[44,45] have demonstrated that mouse αB-crystallin can block okadaic acid and H_2O_2-induced apoptosis in the immortalized rabbit lens epithelial cells, N/N1003A. To delineate the antiapoptotic mechanisms of αA- and αB-crystallins, we utilized our established stable clones, pEGFP-HLE, pEGFP-HαA-HLE and pEGFP-HαB-HLE. After grown to 100% confluence, these cells were subjected to treatment with 100 nM staurosporine for 3, 6, 12 and 17 h. The percentage of apoptotic cells in these samples was analyzed with a viability assay described before.[44,45] As shown in Figure 2a, after a 3 h treatment, about 30% vector-transfected cell underwent apoptosis. In contrast, less than 20% of either HαA- or HαB-transfected cells were apoptotic. A 6 h treatment led to apoptosis of more than 60% of the vector-transfected cells. However, less than 30% of pEGFP-HαA-HLE cells and 25% of pEGFP-HαB-HLE cells were found apoptotic under the same conditions. The apoptotic nature of cell death was verified by DNA fragmentation (Figure 2b). After a 6 h treatment, the DNA from vector-transfected cells displayed a clear pattern of fragmentation (Lane 3 of Figure 2b). However, the DNA samples from either HαA- or HαB-

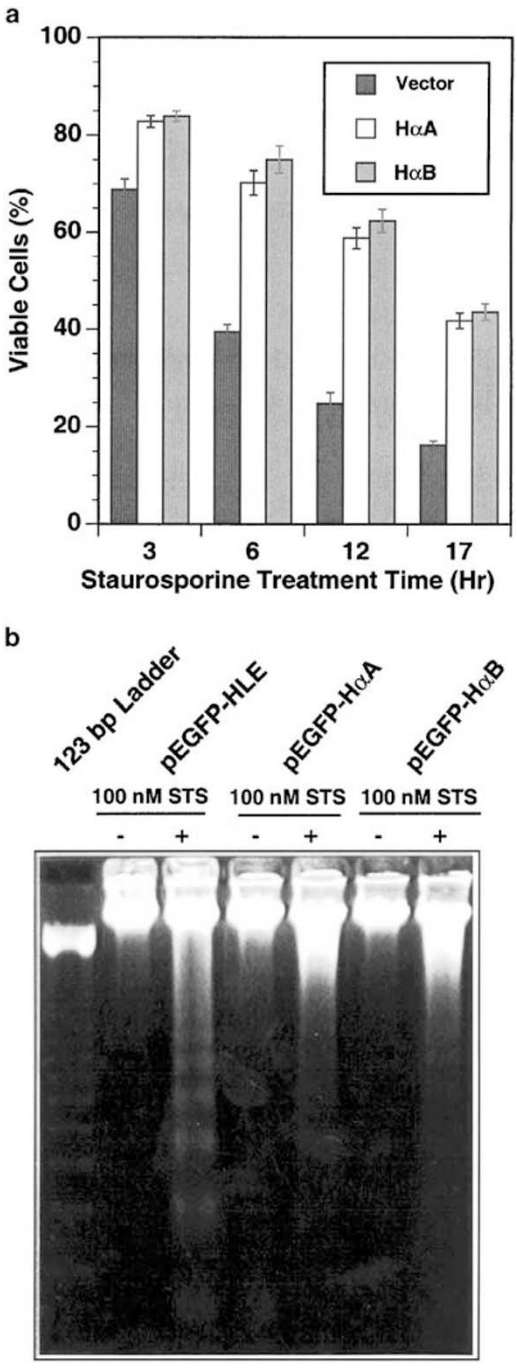

Figure 2 Analysis of the antiapoptotic ability of HαA and HαB in HLE cells. (**a**) Viability assays. pEGFP-HLE, pEGFP-HαA-HLE and pEGFP-HαB-HLE cells were grown to 100% confluence, then treated with 100 nM staurosporine for 3, 6, 12 and 17 h. Viability of the three types of cells was determined as described previously.[99] (**b**) DNA fragmentation assay. pEGFP-HLE, pEGFP-HαA-HLE and pEGFP-HαB-HLE cells were grown to 100% confluence, then treated with 100 nM staurosporine or 0.01% DMSO (control) for 6 h. Then, the cells were harvested for isolation of genomic DNA and the isolated DNA samples were analyzed with 2.0% agarose gel as described previously.[4] The 123 bp marker from Gibco BRL was shown on the left. STS: staurosporine

transfected cells displayed a much weak fragmentation (lanes 5 and 7 of Figure 2b). Thus, HαA- and HαB provide marked protection against staurosporine-induced apoptosis.

HαA- and HαB-crystallins prevent staurosporine-induced upregulation of Bak in human lens epithelial cells

As overexpression of α-crystallins significantly protected HLE cells from staurosporine-induced apoptosis, we first examined whether the antiapoptotic ability of α-crystallins was derived from their regulation of expression of Bcl-2 family members. The pEGFP-HLE, pEGFP-HαA-HLE and pEGFP-HαB-HLE cells were incubated with either 0.01% DMSO or 100 nM staurosporine for 3 h. The total proteins were extracted for Western blot analysis and the results are shown in Figure 3. The relative expression levels of GFP-αA/B-crystallin fusion proteins, Bcl-2, Bcl-X_L, Bcl-X_S, Bax and Bak, were further quantitated using an automated digitizing system from the Silk Scientific Corporation. While expression of Bcl-2, Bcl-X_L, Bcl-X_S and Bax showed only slight variations in vector- and α-crystallin-transfected cells with or without staurosporine treatment (Figure 3 and data not shown), expression of Bak was upregulated about five-fold in vector-transfected cells by staurosporine treatment. In HαA- and HαB-transfected cells, expression of either HαA or HαB enhanced expression of Bak for about 2.5-fold. However, staurosporine-induced additional upregulation was not observed in HαA- and HαB-transfected cells. Thus, HαA and HαB were able to suppress staurosporine-induced upregulation of Bak in HLE cells.

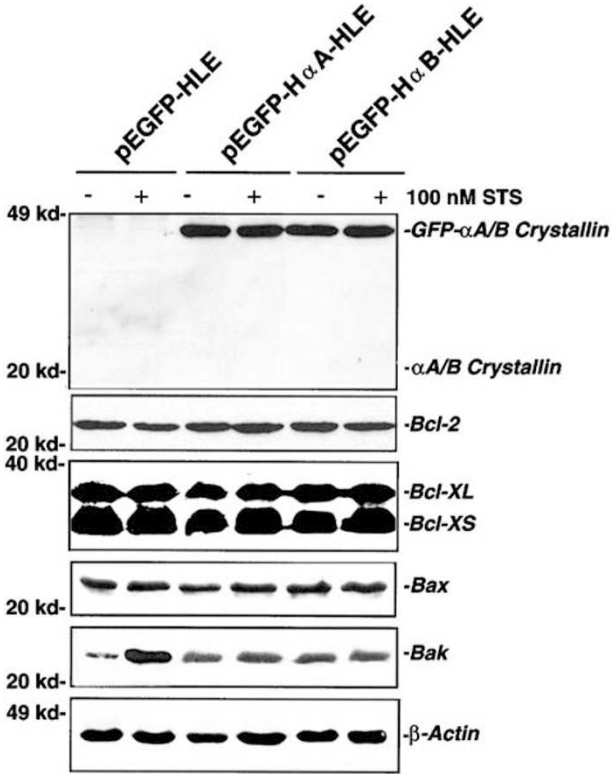

Figure 3 Expression of different Bcl-2 family members during staurosporine-induced apoptosis. The pEGFP-HLE, pEGFP-HαA-HLE and pEGFP-HαB-HLE cells were treated with either 0.01% DMSO (−STS) or 100 nM staurosporine (+STS) for 3 h. The total proteins from the differentially treated cells were extracted and analyzed by Western blot analysis with anti-αA/B-crystallin, anti-Bcl-2, anti-Bcl-$X_{S/L}$, anti-Bax, anti-Bak and anti-β-actin antibodies as described in the Material and Methods

HαA- and HαB-crystallins can interact with Bcl-X_S and Bax *in vitro* and *in vivo*

To explore whether αA- and αB-crystallins are able to prevent apoptosis at the mitochondrial level, upstream of caspase-3 activation, as part of the antiapoptotic mechanism, we conducted GST pulldown assays to identify possible interactions between HαA-crystallin as well as HαB-crystallin with members of the Bcl-2 family. The cDNAs for HαA- and HαB-crystallins were subcloned into pGEX-4T-1 vector to establish (in frame) GST-HαA- and GST-HαB-crystallin fusion protein constructs. The purified GST-HαA- and GST-HαB-crystallin fusion proteins from *Escerichia coli* BL21 were used to pull down the HαA- and HαB-crystallins-associated proteins from HLE cells. The proteins pulled down were further analyzed with antibodies against various members of the Bcl-2 family. As shown in Figure 4, both Bax (the third panel from top) and Bcl-X_S (the fourth panel from the top) were found bound to GST-HαA- and GST-HαB-crystallins, but not to the GST protein control. In contrast, the anti-Bcl-2 and anti-Bak antibodies did not crossreact with any proteins eluted from either GST-HαA or GST-HαB columns (the top two panels of Figure 4). To confirm that the interaction actually occurs *in vivo*, coimmunoprecipitates from the pEGFP-HLE, pEGFP-HαA-HLE and pEGFP-HαB-HLE cells using anti-αA/B-crystallin antibody were further probed with anti-Bcl-2, anti-Bak, anti-Bax, anti-Bcl-X_S and anti-GFP antibodies (Figure 5a). As expected, anti-Bcl-2 and anti-Bak antibodies did not cross-

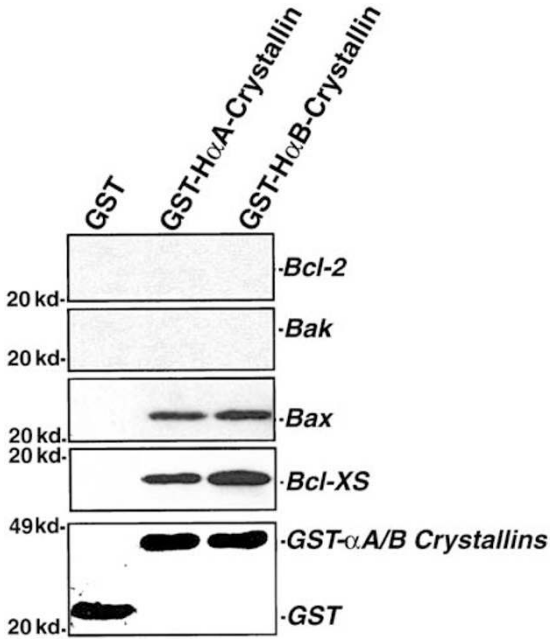

Figure 4 GST pulldown assays to demonstrate that HαA and HαB can interact with Bax and Bcl-X_S *in vitro*. The purified GST, GST-HαA and GST-HαB fusion proteins immobilized on glutathione–Sepharose beads were incubated with cell extracts from the HLE cells. After removal of nonspecific proteins by tris-buffered saline with tween-20 (TBS-T) washes, the associated proteins were eluted and separated by 10% SDS polyacrylamide gel electrophoresis (PAGE). The immunoblots were probed with the antibodies against different members of the Bcl-2 family as indicated in the figure. Only Bax and Bcl-X_S were found bound to HαA and HαB. The lower panel shows equal input of GST, GST-HαA and GST-HαB

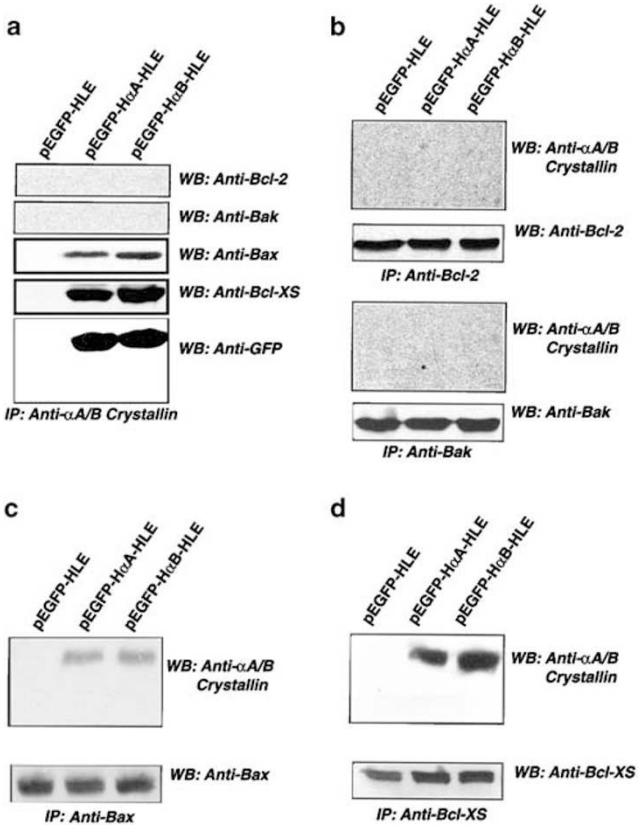

Figure 5 Coimmunoprecipitations to demonstrate that HαA and HαB can interact with Bax and Bcl-X_S *in vivo*. (**a**) The total proteins extracted from pEGFP-HLE, pEGFP-HαA-HLE and pEGFP-HαB-HLE cells were immunoprecipitated with anti-αA/B-crystallin antibody. The precipitated samples were then sequentially blotted with anti-Bcl-2, anti-Bak, anti-Bax, anti-Bcl-X_S and anti-GFP antibodies. Only Bax and Bcl-X_S were found to be brought down by anti-αA/B-crystallin antibody. (**b**) The total proteins extracted from pEGFP-HLE, pEGFP-HαA-HLE and pEGFP-HαB-HLE cells were immuoprecipitated by anti-Bcl-2 and anti-Bak antibodies. The precipitated samples were then probed with both anti-αA/B-crystallin antibody and anti-Bcl-2 (top two panels) or anti-αA/B-crystallin antibody and anti-Bax antibodies (bottom two panels). Note that there was no crossreacting protein detected with anti-αA/B-crystallin antibody in both samples brought down either by anti-Bcl-2 or by anti-Bak antibodies. (**c**) The total proteins extracted from pEGFP-HLE, pEGFP-HαA-HLE and pEGFP-HαB-HLE cells were immunoprecipitated using anti-Bax antibody. The precipitated samples were then sequentially probed with anti-αA/B-crystallin and anti-Bax antibodies. (**d**) The total proteins extracted from pEGFP-HLE, pEGFP-HαA-HLE and pEGFP-HαB-HLE cells were immuoprecipitated using anti-Bcl-X_S antibody. The precipitated samples were then sequentially blotted with anti-αA/B-crystallin and anti-Bcl-X_S antibodies

react with any proteins precipitated down by anti-αA/B-crystallin antibody (the top two panels of Figure 5a). In contrast, both Bax and Bcl-X_S were coimmunoprecipitated from pEGFP-HαA-HLE and pEGFP-HαB-HLE cells but not from pEGFP-HLE cells using anti-αA/B-crystallin antibody. HαB seemed to have slightly better affinity to Bax and Bcl-X_S than HαA did (the middle two panels of Figure 5a). Since these experiments were semiquantitative, such difference may not be significant. Analysis of Bax and Bcl-X_S left in the supernatant fraction after immunoprecipitation revealed that more than 60% of total Bax and more than 80% of total Bcl-X_S were precipitated down by the anti-αA/B-crystallin antibody (data not shown). Next, we performed the immunoprecipitations with the antibodies against Bcl-2, Bak, Bax and Bcl-X_S and the cell extract from the three types of cells. While anti-Bcl-2 and anti-Bak antibodies did not bring down either GFP-HαA or GFP-HαB (Figure 5b), anti-Bax (Figure 5c) and anti-Bcl-X_S (Figure 5d) antibodies were able to coimmunoprecipitate with GFP-HαA in pEGFP-HαA-HLE cell and GFP-HαB in pEGFP-HαB-HLE cells. In pEGFP-HLE cells, neither HαA nor HαB was detected in the immunoprecipitated proteins by anti-Bax and anti-Bcl-X_S antibodies (left lane of Figure 5c and d). These results indicate that HαA- and HαB can specifically bind to Bax and Bcl-X_S both *in vitro* and *in vivo.*

The N-terminal fragments of HαA and HαB fused with GFP did not protect the transfected cells from apoptosis and displayed no interaction with Bcl-X_S and Bax

To demonstrate that the observed protection against staurosporine-induced apoptosis of pEGFP-HαA-HLE and pEGFP-HαB-HLE cells was not derived from the action of GFP, we have created two fusion protein constructs using PCR cloning strategy. A fragment of 89 amino acids from the N-terminal of HαA was fused with GFP in frame to generate the first construct. Similarly, a fragment of 74 amino acids from the N-terminal of HαB was fused with GFP in frame to create the second construct (Figure 6a). The two constructs were introduced into HLE cells and their expressions were verified by Western blot analysis (Figure 6b) and fluorescence microscopy (Figure 6d and e). Like GFP-HαA and GFP-HαB, the two new fusion proteins, GFP-HαA-89 and GFP-HαB-74, were also distributed in the cytoplasm (Figures 6d and e). Treatment of the cells expressing these new fusion proteins with 100 nM staurosporine induced apoptosis of similar rate as found in vector-transfected cells (Figure 6f), indicating the absence of protection by these new fusion proteins. Immunoprecipitation with anti-GFP, anti-Bax and anti-Bcl-X_S antibodies on the total proteins extracted from vector- and the new constructs-transfected cells demonstrated that the two new fusion proteins did not bind to Bax and Bcl-X_S (Figure 6g). Thus, it is the HαA and HαB but not GFP that interacts with Bax and Bcl-X_S.

HαA[R116C] and HαB[R120G] showed much less protection on staurosporine-induced apoptosis and also displayed much weak interactions with Bcl-X_S and Bax

Two major mutants found in α-crystallin are R116C in HαA and R120G in HαB. Previous studies[73,74] have shown that both mutants displayed decreased protection against apoptosis induced by staurosporine and other stress conditions. To explore the possible mechanisms for the decreased protection, we have created the two mutants using wild-type HαA and HαB cDNAs and PCR amplification procedure. The two mutants were fused into the GFP expression vector to generate pEGFP-HαA[R116C] and pEGFP-HαB[R120G], which were introduced into HLE cells. Expressions of HαA[R116C] and HαB[R120G] were confirmed with Western blot analysis (Figure 7a). Their protections against stauro-

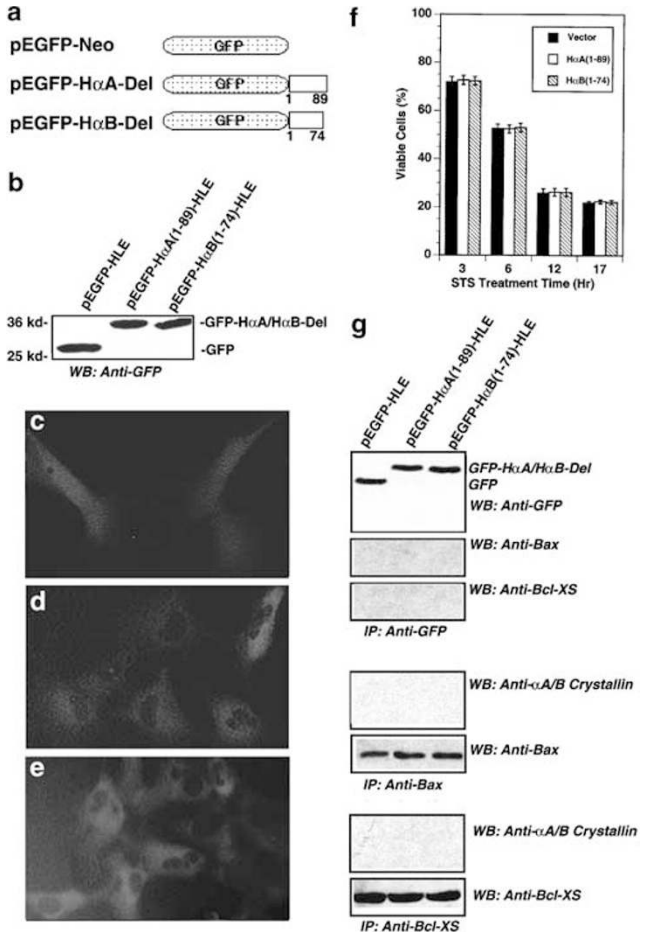

Figure 6 Demonstration that the N-terminal fragments of either HαA or HαB, when fused with GFP, was also localized in the cytoplasm but displayed no protection against staurosporine-induced apoptosis. (**a**) Diagram of the structures of pEGFP-neo, pEGFP-HαA-Del and pEGFP-HαB-Del. (**b**) Western blot analysis of expression of GFP, GFP-HαA-Del and GFP-HαB-Del. Western blot analysis was carried out as described in Figure 1. (**c–e**) Detection of GFP, GFP-HαA-Del and GFP-HαB-Del by fluorescence microscopy as described in Figure 1. (**f**). HαA-Del- and HαB-Del-transfected cells displayed similar apoptosis rate as vector-transfected cells. Viability was assayed as described in Figure 2a. (**g**) Coimmunoprecipitations revealed that these deletion mutants of HαA and HαB do not interact with Bax and Bcl-X_S. Coimmunoprecipitation was conducted as described in Figure 5.

sporine-induced apoptosis were analyzed. As shown in Figure 7b, both HαA[R116C] and HαB[R120G] displayed less protection against staurosporine-induced apoptosis as compared with wild-type HαA and HαB (Figure 2a). To explore the possible mechanism for this decreased antiapoptotic ability, we examined their interactions with Bax and Bcl-X_S. Reciprocal immunoprecipitation with anti-αA/B-crystallin, anti-Bax and anti-Bcl-X_S antibodies revealed that HαA[R116C] and HαB[R120G] had much weaker interactions with both Bax and Bcl-X_S in comparison with the corresponding wild-type proteins, HαA and HαB (Figure 7c). Thus, part of the mechanisms responsible for the decreased protection by HαA[R116C] and HαB[R120G] are derived from their aberrant interactions with the two proapoptotic members of the Bcl-2 family.

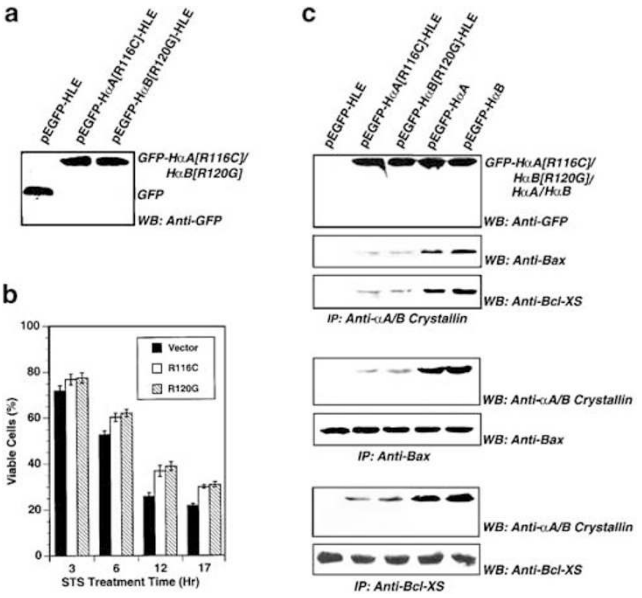

Figure 7 Demonstration that R116C and R120G, the two major mutant proteins found in HαA and HαB, have decreased ability against staurosporine-induced apoptosis and also displayed much less affinity for binding to Bax and Bcl-X_S. (**a**) Western blot analysis to detect expressions of GFP, R116C and R120G in pEGFP-HLE, pEGFP-HαA[R116C]-HLE and pEGFP-HαB[R120G]-HLE cells. Western blot analysis was conducted as described in Figure 1. (**b**) Viability assays to show the relative antiapoptotic ability of GFP-R116C and GFP-R120G. Viability assay was conducted as described in Figure 2a. (**c**) Coimmunoprecipitations to demonstrate that R116C and R120G have much lower affinity to Bax and Bcl-X_S in comparison with their wild-type proteins, HαA and HαB. Coimmunoprecipitation was conducted as described in Figure 5

Staurosporine-induced mitochondrial translocations of Bax and Bcl-X_S in pEGFP-HLE cells were blocked in pEGFP-HαA-HLE and pEGFP-HαB-HLE cells

Bcl-2 family members are the major apoptotic regulators that control the homeostasis of mitochondria. Proapoptotic Bcl-2 family members such as Bax and Bcl-X_S have been shown to be activated and translocated from the cytosol into mitochondria after apoptotic stimulation.[24,38] Since human α-crystallins were able to interact with Bax and Bcl-X_S *in vitro* and *in vivo*, we predicted that the translocation of Bax and Bcl-X_S could be affected in the presence of HαA and HαB. To test this possibility, the pEGFP-HLE, pEGFP-HαA-HLE and pEGFP-HαB-HLE cells were treated with either 0.01% DMSO or 100 nM staurosporine for 3 h and the mitochondrial-associated (M) and soluble (S) proteins were isolated from the three types of cells as described in Materials and Methods. Then, the same amounts of mitochondrial (M) and cytosolic proteins (S) were immunoblotted using the antibodies against superoxide dismutase (Mn^{2+}), Bcl-2, Bcl-X_L, Bak, Bax and Bcl-X_S. The purity of mitochondrial fraction was shown by the exclusive distribution of a mitochondria-specific protein, superoxide dismutase (Mn^{2+}) (Figure 8a). Bcl-2, Bcl-X_L and Bak were found to be associated with the mitochondrial membrane even after staurosporine treatment (Figure 8b–d). The upregulated Bak found in pEGFP-HLE cells was also accumulated in the mitochondria (Figure 8d). Bax was distributed in cytosol before staurosporine treatment in all

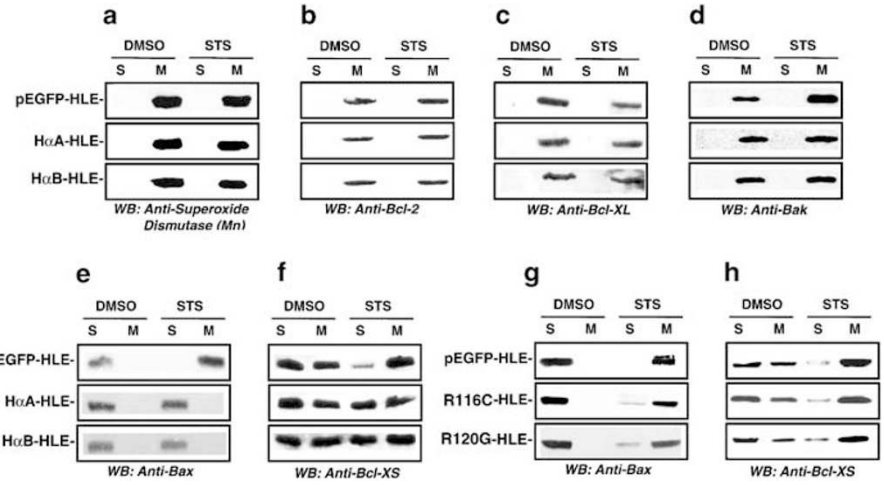

Figure 8 Demonstration that HαA and HαB prevent staurosporine-induced translocation of Bax and Bcl-X_S from the cytosol into mitochondria (**a–f**) and that the two mutants, R116C in HαA and R120 in HαB, display much weaker ability to sequester the staurosporine-induced translocation of Bax and Bcl-X_S from the cytosol into mitochondria (**g**–**h**). The pEGFP-HLE, pEGFP-HαA-HLE and pEGFP-HαB-HLE cells were grown to 100% confluence and then treated with 0.01% DMSO (DMSO) or 100 nM staurosporine (STS) for 3 h. These samples were then used for isolation of mitochondrial (M) and cytosolic (S) fractions. Total proteins were then extracted from the two fractions and subjected to Western blot analysis. Briefly, 50 μg of the mitochondrial protein (M) and cytosolic protein (S) from both control and treated cells were separated by 10% SDS-PAGE. The distributions of Mn-superoxide dismutase (marker for mitochondria-specific protein) (**a**), Bcl-2 (**b**), Bcl-X_L (**c**), Bak (**d**), Bax (**e**) and Bcl-X_S (**f**) were determined by Western blot analysis using the corresponding antibodies. Similarly, the pEGFP-HLE, pEGFP-HαA[R116C]-HLE and pEGFP-HαB[R120G]-HLE cells were grown to 100% confluence and then treated with 0.01% DMSO (DMSO) or 100 nM staurosporine (STS) for 3 h. These samples were then used for isolation of mitochondrial (M) and cytosolic (S) fractions. Total proteins were then extracted from the two fractions and subjected to Western blot analysis using antibody against Bax (**g**) and Bcl-X_S (**h**) as described above. Note that R116C and R120G display much weaker ability to sequester Bax (**g**) and Bcl-X_S (**h**) in the cytosol compared with the sequestration of Bax (**e**) and Bcl-X_S (**f**) by wild-type HαA and HαB

three types of cells. However, after staurosporine treatment, Bax was translocated into mitochondria in pEGFP-HLE cells but retained in cytosol of pEGFP-HαA-HLE and pEGFP-HαA-HLE cells (Figure 8e). Bcl-X_S was equally distributed in both the soluble fraction (S) and the mitochondria-associated fraction (M) before staurosporine treatment. After treatment with 100 nM staurosporine, more than 90% of Bcl-X_S was translocated into mitochondria, leading to its dominant distribution in mitochondria and much less amount in the cytosolic fraction in pEGFP-HLE cells (top panel of Figure 8f). In contrast, in pEGFP-HαA-HLE cells (middle panel of Figure 8f) and pEGFP-HαB-HLE cells (bottom panel of Figure 8f), the staurosporine-induced translocation of Bcl-X_S was largely blocked as reflected by the even distribution of Bcl-X_S in both cytosolic fraction and mitochondria with or without 100 nM staurosporine treatment. In contrast, the two prominent mutants, R116C and R120G, displayed much weaker abilities to sequester Bax (Figure 8g) and Bcl-X_S (Figure 8h) in the cytosol. These results demonstrated that HαA and HαB can prevent the translocation of Bcl-X_S and Bax into mitochondria after staurosporine stimulation.

HαA and HαB prevent staurosporine-induced cytochrome *c* release, caspase-3 activation and PARP cleavage

Earlier studies have shown that translocation of Bax directly induces release of cytochrome *c* from mitochondria and activation of caspase-3.[30–31] As HαA and HαB can interact with Bax and Bcl-X_S and prevent their translocation from the cytosol to mitochondria, we tested whether this sequestration could inhibit release of cytochrome *c* and suppress activation of caspase-3. Total proteins from both the cytosolic fraction and mitochondria of the three types of cells treated with 0.01% DMSO or 100 nM staurosporine for 0.5, 3 and 6 h were analyzed with Western blot analysis using an anti-cytochrome *c* antibody. As shown in Figure 9a, after 30-min treatment by staurosporine, no cytochrome *c* was released from either vector- or HαA- or HαB-transfected cells. As the treatment time increased to 3 h, staurosporine induced a substantial amount of cytochrome *c* released from mitochondria (M) into cytosol (S) in pEGFP-HLE cells (Figure 9b, top panel). However, the release of cytochrome *c* was hardly observed in either HαA- or HαB-transfected HLE cells (Figure 9b, middle and bottom panels). By 6 h treatment, a majority of cytochrome *c* was released into cytoplasm in vector-transfected cells (Figure 9c, top panel). In contrast, only a small amount of cytochrome *c* was released in HαA- and HαB-transfected HLE cells (Figure 9c, middle and bottom panels). Since differential release of cytochrome *c* was observed in the three types of cells, we predicted that activation of caspase-3 and downstream apoptotic events may also be different in these cells. To test this possibility, total proteins from these cells treated with either 0.01% DMSO or 100 nM staurosporine for 6 h were extracted for analysis of caspase-3 activity and cleavage of poly (ADP-ribose) polymerase (PARP), a substrate of caspase-3. As shown in Figure 10a, staurosporine treatment of pEGFP-HLE cells induced more than 17-fold activation of caspase-3 compared with DMSO treatment. In contrast, only two- to three-fold activation induced by staurosporine was observed in pEGFP-HαA-HLE and pEGFP-HαB-HLE cells in comparison with DMSO treatment. Consistent with differential caspase-3 activation, a large amount of PARP p116 was

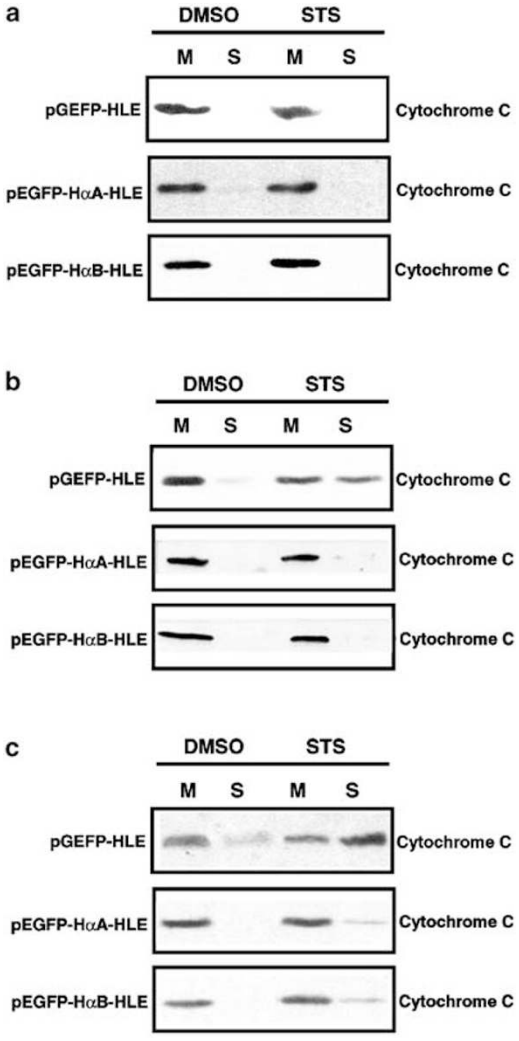

Figure 9 Demonstration that HαA and HαB prevent staurosporine-induced release of cytochrome *c*. The pEGFP-HLE, pEGFP-HαA-HLE and pEGFP-HαB-HLE cells were grown to 100% confluence and then treated with 0.01% DMSO (control) or 100 nM staurosporine (STS) for 30 min (**a**), 3 h (**b**) and 6 h (**c**). These samples were then used for isolation of mitochondrial (M) and cytosolic (S) fractions. Total proteins were then extracted from the two fractions and subjected to Western blot analysis. Briefly, 50 μg of the mitochondrial fraction (M) and cytosolic fraction (S) from the control and treated cells were separated by 10% SDS-PAGE and the immunoblots were detected with an anti-cytochrome *c* antibody

cleaved by caspase-3 to p85 in pEGFP-HLE cells after 6 h treatment by staurosporine. On the other hand, the degraded PARP (p85) was barely detectable in pEGFP-HαA-HLE and pEGFP-HαB-HLE cells (Figure 10b). Thus, both HαA and HαB were able to block downstream apoptotic events through interactions with Bax and Bcl-X_S.

HαA and HαB-crystallins display similar protection against apoptosis induced by different stress conditions in both lens and nonlens cells

Our results with HLE cells under treatment of 100 nM staurosporine suggest that HαA and HαB display similar protection against induced apoptosis. To further confirm these

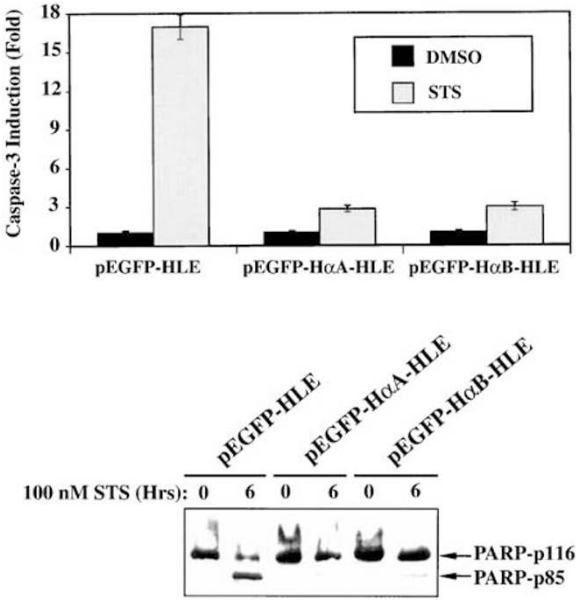

Figure 10 Demonstration that HαA and HαB prevent staurosporine-induced activation of caspase-3 and cleavage of PARP. (**a**) Caspase-3 activity in pEGFP-HLE, pEGFP-HαA-HLE and pEGFP-HαB-HLE cells after treatment with 0.01% DMSO (DMSO) or 100 nM staurosporine (STS). Caspase-3 activity was analyzed as described previously.[44,45] Note that staurosporine induced more than 17-fold increase in caspase-3 activity compared to the DMSO control in vector-transfected cells. The activation of caspase-3 in HαA- and HαB-transfected cells was substantially repressed. (**b**) Western blot analysis of the caspase-3 substrate, PARP. Nuclear proteins (100 μg) from the pEGFP-HLE, pEGFP-HαA-HLE and pEGFP-HαB-HLE cells after treatment with 0.01% DMSO (control) or 100 nM staurosporine(STS) for 6 h were separated in an 8% SDS polyacrylamide gel. The PARP cleavage was detected with an anti-PARP antibody. Note that the p85 subunit was prominent in vector-transfected cells but barely detectable in HαA- and HαB-transfected cells after 100 nM staurosporine treatment

results, we introduced both HαA and HαB into a retina pigment epithelial cell line, ARPE-19,[75] and a rat embryonic myocardium cell line, H9c2.[76] Different from the SV40 large T-transformed HLE cells that lack endogenous α-crystallin, both ARPE-19 and H9c2 express endogenous αB-crystallin. ARPE-19 cells expressed about 0.4 ng αB-crystallin/μg total proteins using purified αB-crystallin (Stressgen) as standard. The rat embryonic myocardium, H9c2 cells, expressed 0.21 ng αB-crystallin/μg total proteins, half of that found in ARPE-19 cells (data not shown). Accordingly, both ARPE-19 and H9c2 have much stronger resistance to staurosporine-apoptosis in comparison with HLE cells in the absence of the exogenous α-crystallin expression (see the vector-transfected cells in Figure 11a, c and e). We suggest that different expression levels of the endogenous αB-crystallin levels likely contribute to their differential antiapoptotic abilities of ARPE-19 and H9c2 cells (see the vector-transfected cells in Figure 11c and e). Expression of the exogenous GFP-HαA or GFP-HαB fusion protein in both ARPE-19 and H9c2 cells provides additional protection (Figure 11c–f). When the established stable clones of vector or human α-crystallin-transfected ARPE and H9c2 cells (those clones expressing similar levels of GFP, GFP-HαA or GFP-HαB were used) were subjected to treatment of 100 nM staurosporine (Figure 11c and e), 10 μM etoposide (Figure 11d) or 400 mM sorbitol (Figure 11f), it was

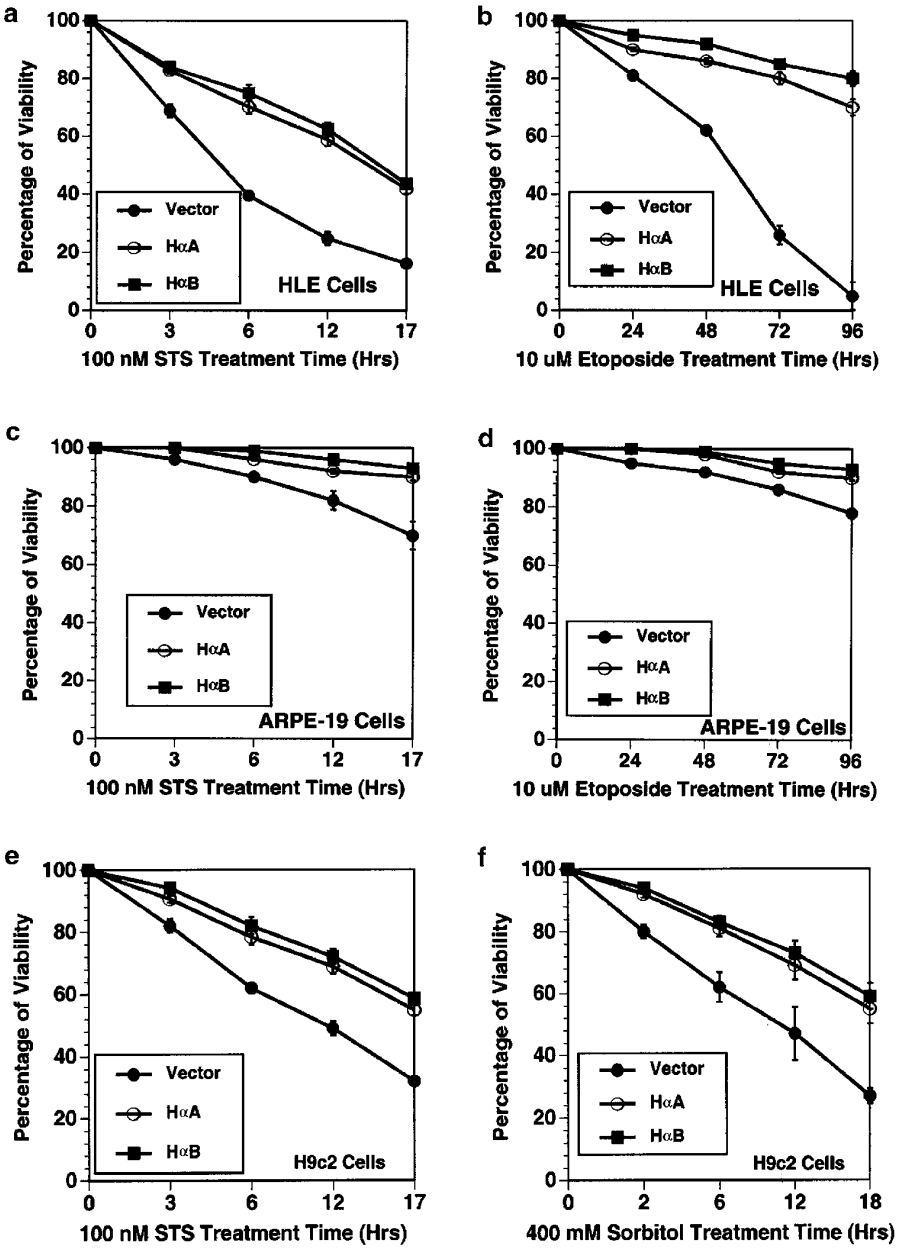

Figure 11 Comparison of the relative antiapoptotic ability of HαA and HαB in three different types of cells. pEGFP-neo, pEGFP-HαA and pEGFP-HαB were introduced into HLE (**a**, **b**), human retina pigment epithelial cells, ARPE-19 (**c, d**) and rat embryonic myocardium cells, H9c2 (**e, f**). After selection with G418 medium, stable clones expressing GFP, GFP-HαA or GFP-HαB were isolated. Their expression levels were determined by Western blot analysis. For all cells (HLE or ARPE-19 or H9c2), the clones with similar expression levels were used for analysis of the relative ability against induced apoptosis. Each stable clone was grown to 100% confluence and then subjected to treatment by 100 nM staurosporine (**a, c, e**), or 10 μM etoposide (**b**, **d**), or 400 mM sorbitol (**f**) for different length of time as indicated, the viability was then assayed as described in Figure 2a

found that both HαA and HαB displayed similar protection against all stress conditions tested (Figure 11).

Discussion

In the present study, we have demonstrated the following: (1) both GST pulldown assay and coimmunoprecipitation demonstrate that HαA and HαB binds to Bax and Bcl-X_S; (2) the two prominent mutants, R116C in HαA and R120G in HαB, display much weaker affinity to Bax and Bcl-X_S; (3) the interactions between α-crystallin and Bax as well as Bcl-X_S prevent their translocation into mitochondria during staurosporine-induced apoptosis; (4) the two prominent mutants, R116C and R120G, exhibit much attenuated sequestration of Bax and Bcl-X_S in the cytosol; (5) both HαA and HαB display similar antiapoptotic ability as tested in three different cell lines under various stress conditions; (6) through inhibition of Bax and Bcl-X_S translocation and repression of Bak upregulation, HαA and HαB prevent staurosporine-induced apoptosis. Thus, our results reveal a novel antiapoptotic mechanism for α-crystallin (Figure 12).

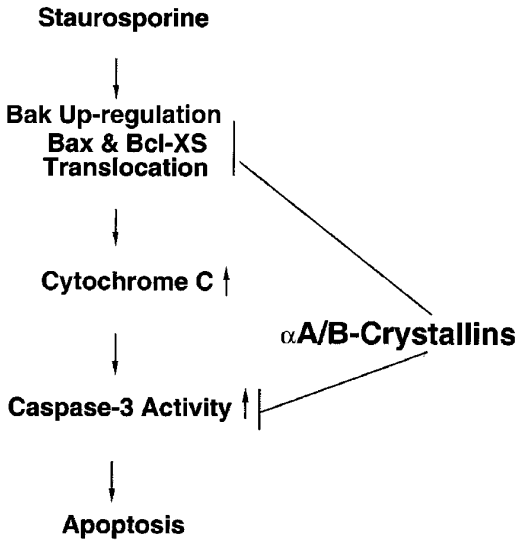

Figure 12 Diagram to show the apoptotic pathway for staurosporine-induced apoptosis in HLE cells and the protective mechanisms of HαA and HαB against staurosporine-induced apoptosis. Staurosporine induces upregulation of Bak and translocation of Bax and Bcl-X_S, leading to alteration in the permeability of mitochondria as reflected by release of cytochrome *c*, which causes activation of caspase-3 and cleavage of PARP, and eventually execution of the apoptotic program. HαA and HαB block upregulation of Bak and translocation of Bax and Bcl-X_S, and consequently suppress downstream apoptotic events

Antiapoptotic mechanisms of α-crystallins

The small heat-shock proteins have multiple functions.[39–46, 62–74] One of the most important functions is the ability to protect cell from induced apoptosis.[39–46] α-Crystallin and Hsp27 are closely related family members and protect cells from apoptosis induced by a large numbers of stress factors.[39–46] Both of them prevent stress-induced apoptosis at multiple signaling steps. However, the exact mechanism or regulating targets seem to be different. Hsp27 prevents apoptosis by interacting with caspase-3 to modulate its activity,[47–48] by interacting with cytochrome *c* to prevent procaspase-9 activation,[49] or by regulating Bid intracellular distribution and F actin integrity to block mitochondrial death pathway.[52] In contrast, α-crystallin utilizes a different mechanism to negatively regulate caspase-3 activity. Our recent study shows that αB-crystallin prevents H_2O_2-induced apoptosis through interaction with procaspase-3 and partially processed procaspase-3 to prevent caspase-3 activation.[45] Secondly, instead of regulating Bid distribution, our results presented here demonstrate that α-crystallin binds to Bax and Bcl-X_S to prevent their translocation into mitochondria induced by staurosporine, thus maintaining the integrity of mitochondria. The differential antiapoptotic mechanism was further illustrated in a recent study in which αB-crystallin but not Hsp27 was found capable of repressing differentiation-induced caspase-3 activation.[74]

The results from both GST pulldown assay (Figure 4) and coimmunoprecipication-linked Western blot analysis with antibodies against αA/B-crystallin and Bcl-X_S (Figure 5a and d) suggest that HαB seems to have slightly stronger affinity to Bax and Bcl-X_S than HαA does. However, this is not consistent with the coimmunoprecipitation-linked Western blot analysis with anti-Bax antibody (Figure 5c). Such discrepancy may be partially derived from the difference in the antibody affinity to the complexes precipitated and also partially resulted from variation from experiments to experiments (Figure 5c and Figure 7c). Since both assays are semiquantitative, the observed differential affinity to Bax and Bcl-X_S displayed by HαA and HαB need to be further explored. Nevertheless, our observation that both HαA and HαB bind to these proapoptotic regulators and sequester their translocation into mitochondria during staurosporine-induced apoptosis is important for understanding the antiapoptotic mechanisms of HαA and HαB.

The two major mutants, R116C in HαA and R120G in HαB, cause cataractogenesis in the lens.[77,78] Consistent with these observations, the chaperone-like ability of R116C and R120G was found substantially decreased.[79,80] The results reported here and also from earlier studies[73–74] reveal that the two mutants apparently display much weaker antiapoptotic ability. Our demonstration that the mutants have much less affinity to Bax and Bcl-X_S provides an explanation. Part of their attenuated antiapoptotic ability is derived from their weak interactions with Bax and Bcl-X_S and thus decreased ability to sequester translocation of Bax and Bcl-X_S from cytosol into mitochondria induced by staurosporine treatment. Why R116C and R120G display deceased affinities to Bax and Bcl-X_S remains to be further studied.

An early study[43] has suggested that αA-crystallin is more competent than αB-crystallin in preventing apoptosis induced by staurosporine, TNF-α and UVA. In the present study, we have compared the antiapoptotic ability of the two crystallins in three different cell lines: the human lens epithelial cell line (HLE) which contains virtually undetectable endogenous crystallins; the human retina pigment epithelial cells (ARPE-19) and the rat embryonic myocardium cell line (H9c2), both of which expresses endogenous αB-crystallin. The expression of the endogenous αB-crystallin in ARPE-19 and H9c2 cells makes them much more resistant to staurosporine-induced apoptosis in the absence of exogenous α-crystallin expression (Figure 11). Regardless absence or presence of the endogenous α-crystallin, expression of HαA and HαB in these cells provides additional protections. Under treatment of 100 nM staurosporine, 10 μM etoposide or 400 mM sorbitol (generating osmotic stress), HαA and HαB consistently show similar protections against a given stress condition in HLE, ARPE-19 or H9c2 cells.

Signaling pathway mediating staurosporine-induced apoptosis

Apoptosis occurs through two major signaling pathways: extrinsic or intrinsic.[81] The extrinsic pathway initiated from activation of death domain containing cell surface receptors of the tumor necrosis factor (TNF) super family leads to the recruitment and proteolytic activation of caspase-8, which results in the cleavage and activation of downstream effector caspases.[82–83] The intrinsic apoptotic signaling pathway involves mitochondria and results in the release of proapoptotic factors from mitochondria, such as cytochrome *c*. The released cytochrome *c* binds to the apoptotic protease-

activating factor-1(Apaf-1), subsequently turns on the downstream executioner caspases such as caspase-3.[84–86] Staurosporine, a potent apoptosis inducer demonstrated in a broad spectrum of cells activate apoptosis through the mitochondrial death pathway.[87–91] The proapoptotic members of the Bcl-2 family play a critical role in staurosporine-induced apoptosis. Cells lacking both Bax and Bak are known to be completely resistant to multiple apoptotic stimuli including staurosporine.[92–93] Analysis of cell death in Bax- or Bak-deficient cell lines indicates that both regulators are necessary for staurosporine-induced apoptosis.[94,95] Consistent with these studies, here we show that in HLE cells staurosporine regulates both Bak and Bax at different ways.

Staurosporine was found to upregulate Bak expression up to five-fold (Figure 3) and the upregulated Bak was accumulated into mitochondria (Figure 8) in vector-transfected cells. In the HαA- and HαB-transfected cells, Bak upregulation is different. First, expression of HαA and HαB enhances Bak expression in unknown mechanism. On the other hand, expression of HαA- and HαB prevents staurosporine-induced additional Bak upregulation (Figure 3). Since cells lacking both Bax and Bak are completely resistant to staurosporine,[92,93] inhibition of additional Bak upregulation by HαA- and HαB, to some degree, contributes to their antiapoptotic abilities against staurosporine-induced apoptosis. Bak upregulation is also observed in human colonic adenoma AA/C1 cells during butyrate-induced apoptosis,[96] and in human stomach epithelial cells during bacterium-induced apoptosis.[97]

It is well established that death signal induced conformation change followed by insertion into mitochondrial membrane is an important step for Bax to promote apoptosis.[25–28] Although staurosporine does not induce Bax upregulation, this kinase inhibitor promotes Bax translocation from cytosol into mitochondria in vector-transfected cells, thus turning on the mitochondrial death pathway. This process is largely abrogated in cells expressing either HαA or HαB (Figure 8e).

In addition, our results demonstrate that staurosporine also regulates Bcl-X_S. It also stimulates translocation of Bcl-X_S from cytosol into mitochondria in vector-transfected pEGFP-HLE cells. To our knowledge, this is the first evidence that Bcl-X_S translocation is stimulated by staurosporine. Again, HαA and HαB prevent translocation of Bcl-X_S (Figure 8f).

In vector-transfected cells, once the proapoptotic members, Bax and Bcl-X_S, were mobilized into mitochondria, the integrity of mitochondria was interrupted as evidenced by the release of cytochrome *c*, followed by activation of executioner caspase, caspase-3 and degradation of PARP. These downstream events induced by staurosporine in vector-transfected HLE cells are similar to those reported in other cell lines.[87–91] In either HαA- or HαB-transfected cells, the staurosporine-induced downstream events were largely turned off. Thus, our results provide additional evidence that both Bax and Bak are important for staurosporine-induced apoptosis. Moreover, our demonstration that staurosporine stimulates translocation of Bcl-X_S provides novel information for our understanding of staurosporine-induced signaling pathway (Figure 12).

Materials and Methods

Chemicals

Various molecular biology reagents were purchased from Invitrogen Life Technologies, Gaithersburg, MD, USA; Stratagene, La Jolla, CA, USA and Promega Biotech, Madison, WI, USA. All the oligos, DNA and protein size markers were purchased from Invitrogen Life Technologies, Gaithersburg, MD, USA. Mammalian expression vector was purchased from Clontech, Palo Alto, CA, USA. Various antibodies were obtained from Cell Signaling Technology, Boston, MA, USA; Roche Molecular Biochemicals, Indianapolis, IN, USA; Transduction Laboratories, San Diego, CA, USA and Stressgen, Vancouver, Canada. The culture medium, and most other chemicals and antibiotics were purchased from Sigma, St. Louis, MO, USA and Invitrogen Life Technologies, Gaithersburg, MD, USA.

Culture of HLE, human retina pigment epithelial cells (ARPE-19) and rat embryonic myocardium cells (H9c2)

The HLE cells, kindly provided by Dr. V Reddy, were grown in Dulbecco's modified Eagle's medium (Gibco catalog number 31600-026) containing 10% fetal bovine serum as described previously.[98] The medium was prepared in ion-exchanged double-distilled water to give an osmolarity of 300 ± 5 mosmol supplemented with 26 mM $NaHCO_3$ and 50 U/ml penicillin and streptomycin. The media and sera were sterilized by filtration through 0.22-μm filters (Corning catalog number 25942) with pH adjusted to 7.2. All cells were kept at 37°C and 5% CO_2 gas phase. The human retina pigment epithelial cells (ARPE-19)[75] and rat embryonic myocardium cells (H9c2)[76] were obtained from ATCC and grown in Eagle's minimal essential medium (MEM) (Fisher Scientific) with addition of 10% fetal bovine serum and 50 U/ml penicillin and streptomycin.

Preparation of expression constructs

The HαA and HαB cDNAs were amplified by RT-PCR from human lens mRNA using the following primers: 5′-TACCTCGAGATGGACGTGACCATCCAGC-3′ (αA-crystallin, forward), 5′-CAACCCGGGTTAGGACGAGGGAGCCGAG-3′ (αA-crystallin, reverse), 5′-TACCTCGAGATGGACATCGCCATCCAC-3′ (αB-crystallin, forward), 5′-CAACCCGGGTTCAAGAAAGGGCATCTA-3′(αB-crystallin, reverse). The cDNAs were further inserted into an enhanced green fluorescence protein expression vector, pEGFPC3, at the *Xho*I and *Sma*I sites that were created by PCR to generate in frame fusion constructs. The pGST-HαA/B-crystallin fusion constructs were created by PCR using the following primers: 5′-TACGAATTCATGGA-CGTGACCATCCAGC-3′ (αA-crystallin, forward), 5′-CAAGTCGACTTAGGACGAGGGA-GCCGAG-3′ (αA-crystallin, reverse), 5′-TACGAATTCATGGACATCGCCATCCAC-3′ (αB-crystallin, forward), 5′-CAAGTCGACTTCAAGAAAGGGCATCTA-3′(αB-crystallin, reverse). The amplified HαA and HαB cDNAs were subcloned into pGEX-4T-1 (Pharmacia Biotech), fused in frame with GST at the *Eco*RI and *Sal*I sites. pEGFP-HαA-Del and pEGFP-HαB-Del were generated using PCR and the following primers: 5′-TACCTCGAGATGGACGTGACCAT-CCAGC-3′ (HαA-Del, forward), 5′-CAAGTCGACCTAGGATCGAACCTCAGAGATG-3′ (HαA-Del, reverse); 5′-TAC-CTCGAGATGGACATCGCCATCCAC-3′ (HαB-Del, forward), 5′- CAAGTCGACC-TATGAGAGTCCAGTGTCAAAC-3′ (HαB-Del, reverse).

In vitro mutagenesis for creation of R116C and R120G mutants

The two prominent mutants R116C and R120G were created through a two-step PCR amplification procedures with the following primers: 5′-TACCTCGAGATGGACGTGA-CCATCCAGC-3′ (R116C, forward-1), 5′-AGCGGCAGTGGAACTCACGGGAAA-3′ (R116C-Reverse-1), 5′-GTTCCACTGCCGCTACCGCCTGCCG-3′ (R116C-forward-2), 5′-CAACC-CGGGTTAGGACGAGGGAGCCGAG-3′ (R116C, reverse-2); 5′-TACCTCGAGATGGACA-TCGCCATCCAC-3′ (R120G forward-1), 5′-ATTTCCCGTGGAACTCCCTGGAGA-3′ (R120G, reverse-1), 5′-GTTCCACGGGAAATACCGGATCCC-3′ (R120G, forward-2), 5′-CAACCCGGGTT-CAAGAAAGGGCATCTA-3′(R120G, reverse-2). For R116C generation, wild-type HαA was used as the template in the initial two PCR reactions. One PCR reaction was conducted with the R116C N-terminal primer pair (forward-1 and reverse-1), and the other conducted with R116 C-terminal primer pair (forward-2 and reverse-2). The products from the two PCR reactions were gel-purified to remove the initial template (HαA full-length cDNA). The recovered two partial cDNAs carrying the mutated codon (from Arg-116 to Cys-116) were first denatured and then annealed together, and the ends are filled with klenow DNA polymerase. The newly annealed mutated cDNA was used for template in the third PCR reaction in which the R116C forward-1 primer, 5′-TACCTCGAGATG-GACGTGACCATCCAGC-3′ and R116C reverse-2 primer, 5′-CAACCCGGGTTAGGACGAGGGAGCCGAG-3′ were used. The amplified cDNA was digested at the *Xho*I and *Sma*I sites and then inserted into the mammalian expression vector pEGFPC3 to produce pEGFP-HαA[R116C]. The same procedure was used to generate pEGFP-HαB[R120G] where the two pairs of R120G primers were used for the PCR reactions. Both pEGFP-HαA[R116C] and pEGFP-HαB[R120G] were sequenced to verify the correct mutation.

Establishment of stable expression cell lines

The pEGFP, pEGFP-HαA and pEGFP-HαB constructs were amplified in DH-5α and purified by two rounds of CsCl ultracentrifugation as previously described.[44,45] Transfection of HLE, ARPE-19 and H9c2 cells was performed using electroporation with a BTX Electro Cell Manipulator as described before[44,45] or with Lipofectamine™ 2000 from the Invitrogen Life Technologies, according to the company instruction manual. The transfected cells were then subjected to G418 (400–600 μg/ml) selection for 4–6 weeks and then the individual clones for the following stable transfected cell lines were established. These include pEGFP-HLE, pEGFP-ARPE-19 and pEGFP-H9c2 (expressing only the GFP from the vector); pEGFP-HαA-HLE, pEGFP-HαA-ARPE-19 and pEGFP-HαA-H9c2 (expressing the fusion protein of GFP-HαA); and pEGFP-HαB-HLE, pEGFP-HαB-ARPE-19, and pEGFP-HαB-H9c2 (expressing the fusion protein of GFP-HαB). pEGFP-HαA[R116C]-HLE, pEGFP-HαA-Del-HLE, pEGFP-HαB[R120G]-HLE and pEGFP-HαB-Del-HLE were also established in the same way using pEGFP-HαA[R116C], pEGFP-HαA-Del, pEGFP-HαB[R120G] and pEGFP-HαB-Del constructs, respectively.

Treatment by staurosporine, etoposide and sorbitol

The pEGFP-HLE, pEGFP-ARPE-19, pEGFP-H9c2, pEGFP-HαA-HLE, pEGFP-HαA[R116C]-HLE, pEGFP-HαA-Del-HLE pEGFP-HαA-ARPE-19, pEGFP-HαA-H9c2, pEGFP-HαB-HLE, pEGFP-HαB[R120G]-HLE, pEGFP-HαB-Del-HLE, pEGFP-HαB-ARPE-19, and pEGFP-HαB-H9c2 cells were grown to 100% confluence in DMEM or MEM containing 10% fetal calf serum in the presence of 400–600 μg/ml G418. Then, the media containing 10% serum plus 0.01% DMSO (control) or 100 nM staurosporine, 10 μM etoposide or 400 mM sorbitol (experiment) were used to replace the culture media for the required period of incubation as indicated. After treatment, all samples were collected for analysis of apoptosis, apoptotic pathways and protein–protein interactions.

Apoptosis assay, DNA fragmentation analysis and Hoechst staining

The percentage of apoptotic cells in DMSO or staurosporine, etoposide or sorbitol-treated samples was determined as described before.[99] The apoptotic nature of the treated cells was further verified by DNA fragmentation and Hoechst staining as previously described.[4,44,45,99]

Protein preparation and Western blotting analysis

The total proteins were prepared from the pEGFP-HLE, pEGFP-HαA-HLE, pEGFP-HαB-HLE, pEGFP-HαA[R116C]-HLE, pEGFP-HαB[R120G]-HLE, pEGFP-HαA-Del-HLE and pEGFP-HαB-Del-HLE cells treated with 0.01% DMSO or 100 nM staurosporine for 30 min–6 h using protein extraction buffer. The buffer contained 1% NP-40, 0.5% sodium deoxycholate, 0.1% SDS, 9.1 mM Na_2HPO_4, 1.7 mM NaH_2PO_4, 150 mM NaCl, 10 μl/ml phenylmethylsufonyl fluoride (PMSF) stock solution (10 mg/ml in isopropanol), 30 μl/ml aprotinin with pH of the preparation adjusted to 7.4. After homogenization by passing through a 21-gauge needle, an additional 10 μl of PMSF was added to each sample, which was incubated on ice for 30 min. After the cell lysate was centrifuged at 10 000 × *g* for 20 min at 4°C, the supernatant fraction of each sample was collected and stored in aliquots at −70°C. For each sample, the protein concentration was determined as previously described.[44,45] In total, 50 or 100 μg of total proteins in each sample were resolved by 10% SDS-polyacrylamide gel and transferred into supported nitrocellulose membranes. The protein blots were blocked with 5% nonfat milk in tris-buffered saline (TBS) (10 mM Tris HCl, pH 8.0/150 mM NaCl) overnight at 4°C, and incubated with anti-αA/B-crystallin antibody (StressGen Biotechnologies), anti-β-actin, anti-Bax, anti-Bcl-$X_{S/L}$, anti-Bcl-2 and anti-cytochrome *c* antibodies (Santa Cruz Biotechnology), anti-Bak antibody (Upstate Biotechnology), anti-PARP antibody and anti-GFP antibody (Roche Molecular Biochemicals) at a dilution of 1:500–2000 (μg/ml) in 5% milk prepared in TBS. The secondary antibody is anti-mouse IgG (for anti-GFP and anti-Bcl-2 antibodies), anti-rabbit IgG (for anti-αA/B-crystallin, anti-Bax, anti-Bcl-$X_{S/L}$, anti-cytochrome *c* and anti-Bak antibodies), or anti-goat IgG (for anti-actin) at a dilution of 1:1000 (Amersham). Immunoreactivity was detected with an enhanced chemilluminescence detection kit according to the company's instruction (ECL, Amersham Corp.).

GST pulldown assay

Human αA- and αB-crystallin cDNAs were subcloned into vector pGEX-4T-1. Both vector and expression constructs were transfected into *E.coli* BL21. When *E.coli* BL21 was grown to $OD_{600} = 0.5$ at 37°C, IPTG was added into the medium to a final concentration of 0.5 mM. The culture was continued overnight at 20°C. Thereafter, cells were harvested by centrifugation, frozen and thawed twice by immersing the tubes in dry ice and a 37°C water bath, and resuspended in 1/50 of the starting culture volume of phosphate-buffered saline (PBS), pH 7.2, 5 mM EDTA, 1 mM dithiothreitol (DTT), 2 μg/ml aprotinin, 2 mM phenylmethylsulfonyl fluoride (PMSF) and 2 mg/ml lysozyme. After 30 min on ice, Triton X-100 was

added to a final concentration of 1% and the cells were sonicated. The supernatant fraction was collected by centrifugation and incubated with the glutathione–Sepharose beads (Sigma) for 1 h. The beads were washed with 1 × PBS, 1% Triton X-100, 5 mM EDTA, 1 mM DTT, 2 μg/ml aprotinin and 1 mM PMSF four times. GST alone, GST-HαA or GST-HαB fusion proteins immobilized on glutathione–agarose beads were incubated with HLE cell lysate overnight at 4°C. The nonspecific binding proteins were washed off the beads with TBST buffer (20 mM Tris-Cl, pH 7.4; 150 mM NaCl; 2 mM EDTA; 1% Triton X-100) four times. The interacting proteins were further analyzed by Western blot using anti-Bax and anti Bcl-X_S antibodies.

Immunoprecipitation-linked Western blot analysis

The pEGFP-HLE, pEGFP-HαA-HLE and pEGFP-HαB-HLE, pEGFP-HαA[R116C]-HLE, pEGFP-HαB[R120G]-HLE, pEGFP-HαA-Del-HLE and pEGFP-HαB-Del-HLE cells were grown to 100% confluence and treated with 0.01%. DMSO or 100 nM staurosporine for 3 h as described above. The treated cells were harvested by the end of treatment and used for extraction of total proteins. The protein samples were quantitated and processed for immunoprecipitation-linked Western blot analysis as described below. First, 500 μg of total proteins from pEGFP-HLE, pEGFP-HαA-HLE and pEGFP-HαB-HLE, pEGFP-HαA[R116C]-HLE, pEGFP-HαB[R120G]-HLE, pEGFP-HαA-Del-HLE and pEGFP-HαB-Del-HLE cells were incubated with 10 μg of antibody against αA/B-crystallins, Bax, Bcl-X_S, Bcl-2 or Bak as well as 50 μl protease inhibitor cocktail for 1 h on ice. After incubation, 50 μl of protein A/G plus agarose were added into each incubated sample. These samples were then incubated overnight in a 4°C refrigerator attached to a slow motion rotator. At the end of incubation, these samples were washed three times with RIPA buffer (1 × PBS, 1% Nonidet P-40, 0.5% sodium deoxycholate, 0.1% SDS) by spinning down for 5 min at 10 000 × *g*. After final wash, the pelleted samples were subjected to Western blot analysis as described above using proper antibodies indicated in the text.

Preparation of mitochondrial and soluble proteins

Preparation of mitochondrial and cytosolic proteins was conducted as described previously.[100] Briefly, 40 dishes (100 mm) of pEGFP-HLE, pEGFP-HαA-HLE and pEGFP-HαB-HLE cells in 100% confluence were treated with 0.01% DMSO or 100 nM staurosporine for 3 h. The cells were harvested and washed twice with PBS. The cell pellets were resuspended in hypotonic buffer (10 mM NaCl, 1.5 mM $MgCl_2$, 10 mM HEPES, pH 7.5) with protease inhibitors and incubated on ice for 30 min. Then the cells were lysed with homogenizers for 20 strokes, and the 4 × MS buffer was added into cell lyses to obtain a final concentration of 1 × MS buffer (110 mM mannitol, 280 mM sucrose, 40 mM HEPES, pH 7.5, 1 mM EDTA, 0.05% BSA, plus protease inhibitors). The cell lysates were centrifuged at 1000 × *g* for 5 min at 4°C to remove nuclei and unbroken cells. The supernatant was further centrifuged at 17 000 × *g* at 4°C for 20 min to separate mitochondrial/heavy membrane fraction and soluble fraction. The mitochodrial/heavy membrane fraction was lysed in protein extraction buffer as described above. The protein concentrations in both fractions were determined as described above. Equal amounts of protein in the mitochondrial/heavy membrane fraction and soluble fraction were separated in 10% SDS-PAGE and assayed by different antibodies as described above. The nuclear proteins were further analyzed with anti-PARP antibody (Pharmingen) to detect PARP cleavage during staurosporine-induced apoptosis.

Acknowledgements

This study was supported in part by the Hormel Foundation, University of Minnesota Graduate School, and NIH Grant EY11372 (DWL). We thank Dr. Venkat Reddy for the human lens epithelial cell line and Dr. Ann Bode for a critical reading of the manuscript. We are also grateful to Ms. Andria Hansen for the editing of the manuscript.

References

1. Li DW-C (1997) The lens epithelium, apoptosis and cataract formation. Nova Acta Leopoldina 75: 81–108
2. Lolley RN (1994) The rd gene defect triggers programmed rod cell death. The Proctor Lecture. Invest. Ophthalmol. Vis. Sci. 35: 4182–4191
3. Papermaster DS and Windle J (1995) Death at an early age. Apoptosis in inherited retina degenerations. Invest Ophthalmol. Vis. Sci. 36: 977–983
4. Li WC, Kuszak JR, Dunn K, Wang RR, Ma W, Wang GM, Spector A, Leib M, Cotliar AM, Weiss M Espy J, Howard G, Farris RL, Auran J, Donn A, Hofeldt A, Mackay C, Merriam J, Mittl R and Smith TR (1995a) Lens epithelial cell apoptosis appears to be a common cellular basis for non-congenital cataract development in humans and animals. J. Cell. Biol. 130: 169–181
5. Li WC, Kuszak JR, Wang G-M, Wu Z-Q and Spector A (1995b) Calcimycin-induced lens epithelial cell apoptosis contributes to cataract formation. Exp. Eye Res. 61: 89–96
6. Li WC and Spector A (1996) Lens epithelial cell apoptosis is an early event in the development of UVB-induced cataract. Free Radic. Biol. Med. 20: 301–311
7. Michael R, Vrensen GF, van Marle J, Gan L and Soderberg PG (1998) Apoptosis in the rat lens after *in vivo* threshold dose ultraviolet irradiation. Invest. Ophthalmol. Vis. Sci. 39: 2681–2687
8. Tamada Y, Fukiage C, Nakamura Y, Azuma M, Kim YH and Shearer TR (2000) Evidence for apoptosis in the selenite rat model of cataract. Biochem. Biophys. Res. Commun. 275: 300–306
9. Yoshizawa K, Oishi Y, Nambu H, Yamamoto D, Yang J, Senzaki H, Miki H and Tsubura A (2000) Cataractogenesis in neonatal Sprague–Dawley rats by *N*-methyl-*N*-nitrosourea. Toxicol. Pathol. 28: 555–564
10. Pandya U, Saini MK, Jin GF, Awasthi S, Godley BF and Awasthi YC (2000) Dietary curcumin prevents ocular toxicity of naphthalene in rats. Toxicol. Lett. 115: 195–204
11. Ye J, Yao K, Lu D, Wu R and Jiang H (2001) Low power density microwave radiation induced early changes in rabbit lens epithelial cells. Chin. Med. J. (Engl) 114: 1290–1294
12. Takamura Y, Kubo E, Tsuzuki S and Akagi Y (2003) Apoptotic cell death in the lens epithelium of rat suger cataract. Exp. Eye Res. 77: 51–57
13. Morgenbesser SD, Schreiber-Agus N, Bidder M, Mahon KA, Overbeek PA, Horner J and DePinho RA (1995) Contrasting roles for c-Myc and L-Myc in the regulation of cellular growth and differentiation *in vivo*. EMBO J. 14: 743–756
14. Gomez Lahoz E, Liegeois NJ, Zhang P, Engelman JA, Horner J, Silverman A, Burde R, Roussel MF, Sherr CJ, Elledge SJ and DePinho RA (1997) Cyclin D- and E-dependent kinases and the p57(KIP2) inhibitor: cooperative interactions *in vivo*. Mol. Cell. Biol. 19: 353–363
15. Yoshida H, Kong YY, Yoshida R, Elia AJ, Hakem A, Hakem R, Penninger JM and Mak TW (1998) Apaf1 is required for mitochondrial pathways of apoptosis and brain development. Cell 94: 739–750
16. Blixt A, Mahlapuu M, Aitola M, Pelto-Huikko M, Enerback S and Carlsson P (2000) A forkhead gene, FoxE3, is essential for lens epithelial proliferation and closure of the lens vesicle. Genes Dev. 14: 245–254
17. Hettmann T, Barton K and Leiden JM (2000) Microphthalmia due to p53-mediated apoptosis of anterior lens epithelial cells in mice lacking the CREB-2 transcription factor. Dev. Biol. 222: 110–123
18. de Iongh RU, Lovicu FJ, Overbeek PA, Schneider MD, Joya J, Hardeman ED and McAvoy JW (2001) Requirement for TGFbeta receptor signaling during terminal lens fiber differentiation. Development 128: 3995–4010
19. Arrigo AP (1998) Small stress proteins: chaperones that act as regulators of intracellular redox state and programmed cell death. Biol. Chem. 379: 19–26

20. Xanthoudakis S and Nicholson DW (2000) Heat-shock proteins as death determinants. Nat. Cell. Biol. 2: E163–E165
21. Gross A, McDonnell JM and Korsmeyer SJ (1999) BCL-2 family members and the mitochondria in apoptosis. Genes Dev. 13: 1899–1911
22. Cory S and Adams JM. (2002) The Bcl2 family: regulators of the cellular life-or-death switch. Nat. Rev. Cancer 2: 647–656
23. Gross A, Jockel J Wei MC and Korsmeyer SJ (1998) Enforced dimerization of BAX results in its translocation, mitochondrial dysfunction and apoptosis. EMBO J. 17: 3878–3885
24. Wolter KG, Hsu YT, Smith CL, Nechushtan A, Xi XG and Youle RJ (1997) Movement of Bax from the cytosol to mitochondria during apoptosis. J. Cell Biol. 139: 1281–1292
25. Goping IS, Gross A, Lavoie JN, Nguyen M, Jemmerson R, Roth K, Korsmeyer SJ and Shore GC (1998) Regulated targeting of BAX to mitochondria. J. Cell Biol. 143: 207–215
26. Nechushtan A, Smith CL, Hsu YT and Youle RJ (1999) Conformation of the Bax C-terminus regulates subcellular location and cell death. EMBO J. 18: 2330–2341
27. Wang K, Gross A, Waksman G and Korsmeyer SJ (1998) Mutagenesis of the BH3 domain of BAX identifies residues critical for dimerization and killing. Mol. Cell. Biol. 18: 6083–6089
28. Suzuki M, Youle RJ and Tjandra N (2000) Structure of Bax: coregulation of dimer formation and intracellular localization. Cell 103: 645–654
29. Ghatan S, Larner S, Kinoshita Y, Hetman M, Patel L, Xia Z, Youle RJ and Morrison RS (2000) p38 MAP kinase mediates Bax translocation in nitric oxide-induced apoptosis in neurons. J. Cell. Biol. 150: 335–348
30. Jürgensmeier JM, Xie Z, Deveraux Q, Ellerby L, Bredesen D and Reed JC (1998) Bax directly induces release of cytochrome *c* from isolated mitochondria. Proc. Natl. Acad. Sci. USA 95: 4997–5002
31. Eskes R, Antonsson B, Osen-Sand A, Montessuit S, Richter C, Sadoul R, Mazzei G, Nichols A and Martinou JC (1998) Bax-induced cytochrome *c* release from mitochondria is independent of the permeability transition pore but highly dependent on Mg 2+ ions. J. Cell Biol. 143: 217–224
32. Pastorino JG, Tafani M, Rothman RJ, Marcinkeviciute A, Hoek JB, Farber JL and Marcineviciute A (1999) Functional consequences of the sustained or transient activation by Bax of the mitochondrial permeability transition pore. J. Biol. Chem. 274: 31734–31739
33. Boise LH, Gonzaiz-Garcia M, Postema CE, Ding L, Lindsten T, Turka LA, Mao X, Nunez G and Thompson CB (1993) bcl-x, a bcl-2-related gene that functions as a dominant regulator of apoptotic cell death. Cell 74: 597–608
34. Clarke MF, Apel IJ, Benedict MA, Eipers PG, Sumantran V, GonzaÂlez-GarcõÂa M, Doedens M, Fukunaga N, Davidson B, Dick JE, Minn AJ, Boise LH, Thompson CB, Wicha M and NuÃez G (1995) A recombinant bcl-xs adenovirus selectively induces apoptosis in cancer cells but not in normal bone marrow cells. Proc. Natl. Acad. Sci. USA 92: 11024–11028
35. Dole MG, Clarke MF, Holman P, Benedict M, Lu J, Jasty R, Eipers P, Thompson CB, Rode C, Bloch C, Nunez and Castle VP (1996) Bcl-xS enhances adenoviral vector-induced apoptosis in neuroblastoma cells. Cancer Res. 56: 5734–5740
36. Pena JC, Fuchs E and Thompson CB (1997) Bcl-x expression influences keratinocyte cell survival but not terminal differentiation. Cell. Growth. Differ. 8: 619–629
37. Kharbanda S, Pandey P, Schofield L, Israels S, Roncinske R, Yoshida K, Bharti A, Yuan ZM, Saxena S, Weichselbaum R, Nalin C and Kufe D (1997) Role for Bcl-x_L as an inhibitor of cytosolic cytochrome *c* accumulation in DNA damage-induced apoptosis. Proc. Natl. Acad. Sci. USA 94: 6939–6942
38. Lindenboim L, Yuan J and Stein R (2000) Bcl-xS and Bax induce different apoptotic pathways in PC12 cells. Oncogene 19: 1783–1793
39. Mehlen P, Kretz-Remy C, Preville X and Arrigo A-P (1996) Human hsp27, Drosophila hsp27 and human alphaB-crystallin expression-mediated increase in glutathione is essential for the protective activity of these proteins against TNFalpha-induced cell death. EMBO J. 15: 2695–2706
40. Mehlen P, Schulze-Osthoff K and Arrigo A-P (1996) Small stress proteins as novel regulators of apoptosis. Heat shock protein 27 blocks Fas/APO-1- and staurosporine-induced cell death. J. Biol. Chem. 271: 16510–16514
41. Golenhofen N, Htun P, Ness W, Koob R, Schaper W and Drenckhahn D (1999) Binding of the stress protein alpha B-crystallin to cardiac myofibrils correlates with the degree of myocardial damage during ischemia/reperfusion *in vivo*. J. Mol. Cell. Cardiol. 31: 569–580
42. Hoover HE, Thuerauf DJ, Martindale JJ and Glembotski CC (2000) Alpha B-crystallin gene induction and phosphorylation by MKK6-activated p38. A potential role for alpha B-crystallin as a target of the p38 branch of the cardiac stress response. J. Biol. Chem. 275: 23825–23833
43. Andley UP, Song Z, Wawrousek EF, Fleming TP and Bassnett S (2000) Differential protective activity of alpha A- and alphaB-crystallin in lens epithelial cells. J. Biol. Chem. 275: 36823–36831
44. Li DW-C, Xiang H, Mao Y-W, Wang J, Fass U, Zhang X-Y and Xu C (2001) Caspase-3 is actively involved in okadaic acid-induced lens epithelial cell apoptosis. Exp. Cell Res. 266: 279–291
45. Mao Y-W, Xiang H, Wang W, Korsmeyer SJ, Reddan J and Li DW-C (2001) Human bcl-2 gene attenuates the ability of rabbit lens epithelial cells against H_2O_2-induced apoptosis through down-regulation of the alpha B-crystallin gene. J. Biol. Chem. 278: 43435–43445
46. Kamradt MC, Chen F and Cryns VL (2001) The small heat shock protein alpha B-crystallin negatively regulates cytochrome *c*- and caspase-8-dependent activation of caspase-3 by inhibiting its autoproteolytic maturation. J. Biol. Chem. 276: 16059–16063
47. Bruey J, Ducasse MC, Bonniaud P, Ravagnan L, Susin SA, Diaz-Latoud C, Gurbuxani S, Arrigo AP, Kroemer G, Solary E and Garrido C (2000) Hsp27 negatively regulates cell death by interacting with cytochrome *c*. Nat. Cell Biol. 2: 645–652
48. Garrido C, Bruey JM, Fromentin A, Hammann A, Arrigo AP and Solary E (1999) HSP27 inhibits cytochrome *c*-dependent activation of procaspase-9. FASEB J. 13: 2061–2070
49. Pandey P, Farber R, Nakazawa A, Kumar S, Bharti A, Nalin C, Weichselbaum R, Kufe D and Kharbanda S (2000) Hsp27 functions as a negative regulator of cytochrome *c*-dependent activation of procaspase-3. Oncogene 19: 1975–1981
50. Tezel G and Wax MB (2000) The mechanisms of hsp27 antibody-mediated apoptosis in retina neuronal cells. J. Neurosci. 20: 3552–3562
51. Wagstaff MJ, Collaco-Moraes Y, Smith J, de Belleroche JS, Coffin RS and Latchman DS (1999) Protection of neuronal cells from apoptosis by Hsp27 delivered with a herpes simplex virus-based vector. J. Biol. Chem. 274: 5061–5069
52. Paul C, Manero F, Gonin S, Kretz-Remy C, Virot S and Arrigo AP (2002) Hsp27 as a negative regulator of cytochrome *c* release. Mol. Cell. Biol. 22: 816–834
53. Beere HM, Wolf BB, Cain K, Mosser DD, Mahboubi A, Kuwana T, Tailor P, Morimoto RI, Cohen GM and Green DR (2000) Heat-shock protein 70 inhibits apoptosis by preventing recruitment of procaspase-9 to the apaf-1 apoptosome. Nat. Cell Biol. 2: 469–475
54. Jäättelä M, Wissing D, Kokholm K, Kallunki T and Egeblad M (1998) Hsp70 exerts its anti-apoptotic function downstream of caspase-3-like proteases. EMBO J. 17: 6124–6134
55. Li C-Y, Lee J-S, Ko Y-G, Kim J-I and Seo J-S (2000) Heat shock protein 70 inhibits downstream of cytochrome *c* release and upstream of caspase-3 activation. J. Biol. Chem. 275: 25665–25671
56. Mosser DD, Caron AW, Bourget L, Denis-Larose C and Massie B (1997) Role of the human heat shock protein hsp70 in protection against stress-induced apoptosis. Mol. Cell. Biol. 17: 5317–5327
57. Takayama S, Bimston DN, Matsuzawa S, Freeman BC, Aime-Sempe C, Xie Z, Morimoto RI and Reed JC (1997) BAG-1 modulates the chaperone activity of Hsp70/Hsc70. EMBO J. 16: 4887–4896
58. Pandey P, Saleh A, Nakazawa A, Kumar S, Srinivasula SM, Kumar V, Weichselbaum R, Nalin C, Alnemri ES, Kufe D and Kharbanda S (2000) Negative regulation of cytochrome *c*-mediated oligomerization of Apaf-1 and activation of procaspase-9 by heat shock protein 90. EMBO J. 19: 4310–4322
59. Xanthoudakis S, Roy S, Rasper D, Hennessey T, Aubin Y, Cassady R, Tawa P, Ruel R, Rosen A and Nicholson DW (1999) Hsp60 accelerates the maturation of pro-caspase-3 by upstream activator proteases during apoptosis. EMBO J. 18: 2049–2056
60. Samali A, Cai J, Zhivotovsky B, Jones DP and Orrenius S (1999) Presence of a pre-apoptotic complex of pro-caspase-3, Hsp60 and Hsp10 in the mitochondrial fraction of jurkat cells. EMBO J. 18: 2040–2048
61. Ingolia TD and Craig EA (1982) Four small Drosophila heat shock proteins are related to each other and to mammalian alpha-crystallin. Proc. Natl. Acad Sci. USA 79: 2360–2364
62. Bloemendal H (1982) Lens proteins. CRC Crit. Rev. Biochem. 12: 1–38

63. Horwitz J (1992) -Crystallin can function as a molecular chaperone. Proc. Natl. Acad. Sci. USA 89: 10449–11045
64. Rao PV, Horwitz J and Zigler Jr JS (1993) Alpha-crystallin, a molecular chaperone, forms a stable complex with carbonic anhydrase upon heat denaturation. Biochem. Biophys. Res. Commun. 190: 786–793
65. Wang K and Spector A (1994) The chaperone activity of bovine alpha crystallin. Interaction with other lens crystallins in native and denatured states. J. Biol. Chem. 269: 13601–13608
66. Boyle D and Takemoto L (1994) Characterization of the alpha-gamma and alpha-beta complex: evidence for an *in vivo* functional role of alpha-crystallin as a molecular chaperone. Exp. Eye Res. 58: 9–15
67. Sun TX, Das BK and Liang JJ (1997) Conformational and functional differences between recombinant human lens alphaA- and alphaB-crystallin. J. Biol. Chem. 272: 6220–6225
68. Kantorow M and Piatigorsky J (1994) Alpha-crystallin/small heat shock protein has autokinase activity. Proc. Natl. Acad. Sci. USA 91: 3112–3116
69. Kantorow M, Horwitz J, van Boekel MA, de Jong WW and Piatigorsky J (1995) Conversion from oligomers to tetramers enhances autophosphorylation by lens alpha A-crystallin. Specificity between alpha A- and alpha B-crystallin subunits. J. Biol. Chem. 270: 17215–17220
70. Aoyama A, Frohli E, Schafer R and Klemenz R (1993) Alpha B-crystallin expression in mouse NIH 3T3 fibroblasts: glucocorticoid responsiveness and involvement in thermal protection. Mol. Cell. Biol. 13: 1824–1835
71. Dasgupta S, Hohman TC and Carper D (1992) Hypertonic stress induces alpha B-crystallin expression. Exp. Eye Res. 54: 461–470
72. Mehlen P, Preville X, Chareyron P, Briolay J, Klemenz R and Arrigo AP (1995) Constitutive expression of human hsp27, Drosophila hsp27, or human alpha B-crystallin confers resistance to TNF- and oxidative stress-induced cytotoxicity in stably transfected murine L929 fibroblasts. J. Immunol. 154: 363–374
73. Andley UP, Patel HC and Xi JH. (2002) The R116C mutation in alpha A-crystallin diminishes its protective ability against stress-induced lens epithelial cell apoptosis. J Biol Chem. 277: 10178–10186
74. Kamradt MC, Chen F, Sam S and Cryns VL. (2002) The small heat shock protein alpha B-crystallin negatively regulates apoptosis during myogenic differentiation by inhibiting caspase-3 activation. J Biol Chem. 277: 38731–38736
75. Dunn KC, Aotaki-Keen AE, Putkey FR and Hjelmeland LM (1996) ARPE-19, a human retina pigment epithelial cell line with differentiated properties. Exp. Eye Res. 62: 155–169
76. Kimes BW and Brandt BL (1976) Properties of a clonal muscle cell line from rat heart. Exp Cell Res 98: 367–381
77. Litt M, Kramer P, LaMorticella DM, Murphey W, Lovrien EW and Weleber RG (1998) Autosomal dominant congenital cataract associated with a missense mutation in the human alpha crystallin gene CRYAA. Hum. Mol. Genet. 7: 471–474
78. Vicart P, Caron A, Guicheney P, Li Z, Prevost MC, Faure A, Chateau D, Chapon F, Tome F, Dupret JM, Paulin D and Fardeau M (1998) A missense mutation in the alphaB-crystallin chaperone gene causes a desmin-related myopathy. Nat. Genet. 20: 92–95
79. Shroff NP, Cherian-Shaw M, Bera S and Abraham EC (2000) Mutation of R116C results in highly oligomerized alpha A-crystallin with modified structure and defective chaperone-like function. Biochemistry 39: 1420–1426
80. Bova MP, Yaron O, Huang Q, Ding L, Haley DA, Stewart PL and Horwitz J (1999) Mutation R120G in alphaB-crystallin, which is linked to a desmin-related myopathy, results in an irregular structure and defective chaperone-like function. Proc. Natl. Acad. Sci. USA 96: 6137–6142
81. Orrenius S, Zhivotovsky B and Nicotera P (2003) Regulation of cell death: the calcium-apoptosis link. Nat. Rev. Mol. Cell. Biol. 4: 552–565
82. Nagata S. (1997) Apoptosis by death factor. Cell 88: 355–365
83. Krueger A, Baumann S, Krammer PH and Kirchhoff S (2001) FLICE-inhibitory proteins: regulators of death receptor-mediated apoptosis. Mol. Cell. Biol. 21: 8247–8254
84. Yang J, Liu X, Bhalla K, Kim CN, Ibrado AM, Cai J, Peng TI, Jones DP and Wang X (1997) Prevention of apoptosis by Bcl-2: release of cytochrome *c* from mitochondria blocked. Science 275: 1129–1132
85. Kluck RM, Bossy-Wetzel E, Green DR and Newmeyer DD (1997) The release of cytochrome *c* from mitochondria: a primary site for Bcl-2 regulation of apoptosis. Science 275: 1132–1136
86. Green DR and Reed JC (1998) Mitochondria and apoptosis. Science 281: 1309–1312
87. Vander Heiden MG, Chandel NS, Williamson EK, Schumacker PT and Thompson CB (1997) Bcl-xL regulates the membrane potential and volume homeostasis of mitochondria. Cell 91: 627–637
88. Bossy-Wetzel E, Newmeyer DD and Green DR (1998) Mitochondrial cytochrome *c* release in apoptosis occurs upstream of DEVD-specific caspase activation and independently of mitochondrial transmembrane depolarization. EMBO J. 17: 37–49
89. Deshmukh M and Johnson Jr EM (2000) Staurosporine-induced neuronal death: multiple mechanisms and methodological implications. Cell Death Differ. 7: 250–261
90. Murphy KM, Ranganathan V, Farnsworth ML, Kavallaris M and Lock RB (2000) Bcl-2 inhibits Bax translocation from cytosol to mitochondria during drug-induced apoptosis of human tumor cells. Cell Death Differ. 7: 102–111
91. Kashkar H, Kronke M and Jurgensmeier JM (2002) Defective Bax activation in Hodgkin B-cell lines confers resistance to staurosporine-induced apoptosis. Cell Death Differ. 9: 750–757
92. Wei MC, Zong WX, Cheng EH, Lindsten T, Panoutsakopoulou V, Ross AJ, Roth KA, MacGregor GR, Thompson CB and Korsmeyer SJ (2001) Proapoptotic BAX and BAK: a requisite gateway to mitochondrial dysfunction and death. Science 292: 727–730
93. Cheng EH, Wei MC, Weiler S, Flavell RA, Mak TW, Lindsten T and Korsmeyer SJ (2001) BCL-2, BCL-X(L) sequester BH3 domain-only molecules preventing BAX- and BAK-mediated mitochondrial apoptosis. Mol. Cell 8: 705–711
94. Wang GQ, Gastman BR, Wieckowski E, Goldstein LA, Gambotto A, Kim TH, Fang B, Rabinovitz A, Yin XM and Rabinowich H (2001) A role for mitochondrial Bak in apoptotic response to anticancer drugs. J. Biol. Chem. 276: 34307–34317
95. Theodorakis P, Lomonosova E and Chinnadurai G (2002) Critical requirement of BAX for manifestation of apoptosis induced by multiple stimuli in human epithelial cancer cells. Cancer Res. 62: 3373–3376
96. Hague A, Diaz GD, Hicks DJ, Krajewski S, Reed JC and Paraskeva C (1997) Bcl-2 and Bak may play a pivotal role in sodium butyrate-induced apoptosis in colonic epithelial cells; however overexpression of bcl-2 does not protect against bak-mediated apoptosis. Int. J. Cancer 72: 898–905
97. Chen G, Sordillo EM, Ramey WG, Reidy J, Holt PR, Krajewski S, Reed JC, Blaser MJ and Moss SF (1997) Apoptosis in gastric epithelial cells is induced by *Helicobacter pylori* and accompanied by increased expression of BAK. Biochem. Biophys. Res. Commun. 239: 626–632
98. Ibaraki N, Chen SC, Lin LR, Okamoto H, Pipas JM and Reddy VN (1998) Human lens epithelial cell line. Exp. Eye Res. 67: 577–585
99. Li DW-C, Fass U, Huizar I and Spector A (1998) Okaidac acid-induced lens epithelial cell apoptosis requires inhibition of phosphatase-1 and is associated with induction of gene expression including p53 and bax. Eur. J. Biochem. 257: 351–361
100. Eskes R, Desagher S, Antonsson B and Martinou JC (2000) Bid induces the oligomerization and insertion of Bax into the outer mitochondrial membrane. Mol. Cell. Biol. 20: 929–935